Hindawi Publishing Corporation
Journal of Nanotechnology
Volume 2014, Article ID 170415, 26 pages
http://dx.doi.org/10.1155/2014/170415

Review Article

Direct-Write Ion Beam Lithography

Alexandra Joshi-Imre[1] and Sven Bauerdick[2]

[1] *Independent, Richardson, TX 75081, USA*
[2] *Raith GmbH, Konrad-Adenauer-Allee 8, Phoenix West, 44263 Dortmund, Germany*

Correspondence should be addressed to Alexandra Joshi-Imre; joshi-imre@alumni.nd.edu

Received 23 July 2013; Revised 22 October 2013; Accepted 27 October 2013; Published 10 February 2014

Academic Editor: Paresh Chandra Ray

Copyright © 2014 A. Joshi-Imre and S. Bauerdick. This is an open access article distributed under the Creative Commons Attribution License, which permits unrestricted use, distribution, and reproduction in any medium, provided the original work is properly cited.

Patterning with a focused ion beam (FIB) is an extremely versatile fabrication process that can be used to create microscale and nanoscale designs on the surface of practically any solid sample material. Based on the type of ion-sample interaction utilized, FIB-based manufacturing can be both subtractive and additive, even in the same processing step. Indeed, the capability of easily creating three-dimensional patterns and shaping objects by milling and deposition is probably the most recognized feature of ion beam lithography (IBL) and micromachining. However, there exist several other techniques, such as ion implantation- and ion damage-based patterning and surface functionalization types of processes that have emerged as valuable additions to the nanofabrication toolkit and that are less widely known. While fabrication throughput, in general, is arguably low due to the serial nature of the direct-writing process, speed is not necessarily a problem in these IBL applications that work with small ion doses. Here we provide a comprehensive review of ion beam lithography in general and a practical guide to the individual IBL techniques developed to date. Special attention is given to applications in nanofabrication.

1. Introduction

The general term "ion beam lithography (IBL)" may be used for two different styles of ion beam processing [1, 2]. The first, referred to as projection IBL, employs a rather broad beam of ions irradiating the sample/wafer through some sort of a mask, with the image formed by the mask demagnified onto the target. The other technique, referred to as direct-write IBL, uses a tightly focused beam of ions to form a scanned ion probe, with position and timing controlled by a pattern generator. Ion beam processing may also be divided based on whether it uses low-mass or large-mass ions, fast or slow ions, or based on the type of ion-matter interaction it employs, that is, milling, etching, deposition, implantation, or other material modifications such as resist exposure. In this paper, we introduce patterning concepts that are relevant to all types of direct-write IBL, although our illustrations will exhibit processing with a focused, low-energy (5–50 kV) Ga^+ beam only, which is the most popular type of direct-write IBL today. In the rest of this paper, the term IBL is used interchangeably with "direct-write IBL" and always refers to the direct-write technique.

The term "focused ion beam (FIB) instrument" reflects a multitude of machines differing not only in the type of their main component, the ion beam, but also in the way the complete instrument setup is constructed. For example, some are specialized to do invaluable work at semiconductor companies assisting the operation of their production line, while others are supremely versatile platforms serving research projects in materials science, physics, biology, or chemical, electrical, and mechanical engineering, and so forth by offering a wide range of analytical and patterning capabilities in a single instrument. Still others are built to provide advanced fabrication capabilities and are based on a dedicated lithography platform with optimized hardware and software components. Today, the number of FIB instruments serving R&D applications worldwide is on the order of 2000 and growing. The number of scientific publications reporting nanofabrication using FIB is also growing steadily.

FIB techniques in nanofabrication owe their success to three key properties. First, the direct nature of processing can greatly simplify sample preparation and thus potentially reduce overall processing time by allowing milling,

deposition, etching, and more in a single instrument. Second, the capability to produce three-dimensional and relatively high aspect ratio structures are of great interest. Third, there is a uniquely minimal, nanoscale interaction volume between impacting ions and the sample material, which is typically a few to tens of nanometer spreading range and penetration depth for 5–50 kV Ga^+ (where the exact numbers are strongly dependent on sample material qualities, too), and this is combined with a large variety of possible interactions (see Section 2). In fact, given all the different potentially available ion-matter interactions that can be confined to such a small volume, the interest in using FIBs in nanofabrication for lithography is expected to rise.

In order to plan nanofabrication processes effectively one must understand the physical nature of FIB patterning, so following this introduction, we first give a brief overview of ion beam and matter interactions and their possible applications in Section 2. This is followed by a review of FIB instruments in Section 3, including short discussions about their components and critical features. Section 4 is dedicated to the introduction of IBL processing parameters and to the most important IBL patterning concepts such as field stitching and pattern overlay. Select applications examples are discussed in Section 5, where brief introductions to most currently pursued IBL techniques are also provided.

2. Ion Beam and Matter Interactions and Their Applications

Dependent on ion energy and the relative masses of the impacting ion and the target (i.e., sample) atoms, different physical phenomena might be dominant in ion-solid interactions (see Giannuzzi and Stevie [3], for an introduction to the three different regimes). The following summary describes the linear collision cascade regime that applies to common FIB operating conditions. When a moderately energetic primary ion strikes a solid target material, it undergoes multiple scattering events, until it loses all its kinetic energy and finally comes to rest implanted in the target material. The scattering events include elastic collisions with the nuclei and inelastic collisions with the electrons of the target material. The atoms that get hit and take up some kinetic energy from the primary ion can also undergo a similar set of scattering events and likely misplace further nuclei until they are stopped. The collision cascade generated this way by a single impacting ion can be modeled as a series of binary collisions, which is the basis of the popular 3D Monte Carlo simulation package SRIM-TRIM [4, 5] (see, e.g., Volkert and Minor [6], for a brief discussion about the collision cascade). The energy loss due to nuclear collisions tends to dominate at the 5–50 keV primary ion energies usually used in FIB technology, which results in a volume of scrambled material and a set of sputtered atoms/ions at the surface around the point of entry (see Orloff et al. [7] for details about scattering theory). Electronic losses contribute mostly to secondary electron emission and electromagnetic radiation and in some cases to phonons or plasmons.

In order to develop a sense of the size and shape of a typical ion-matter interaction volume, take a look at Figure 1, where simulated collision cascades of 5 kV and 30 kV gallium ions in amorphous silicon target material are plotted and compared. The red lines represent the path of primary ions, and the green lines represent the path of misplaced target atoms. Looking at the plots in comparison, it is apparent that a lower energy ion beam both broadens sooner and stops sooner, and it causes less scrambling as well as less sputtering. Sputtering is visible in Figures 1(b) and 1(e) as green recoil trajectories end at the target surface, with the assumption that the kinetic energy carried at this point is still enough to overcome the surface binding energy of the target material and thus the misplaced atom is emitted. As it follows and according to the plots, we could perceive that both the depth and lateral size of the interaction volume for a 5 kV beam are less than half of that for a 30 kV beam; however, these simulations assume ions impacting at a single point and do not deal with ion beam diameters. In reality, lower energy ion beams cannot be focused as tightly as higher energy beams of the same beam current at most practically useful beam currents (dependent on ion source and optics). As a consequence, the interaction volume lateral size for a 30 kV beam can be smaller than that for a 5 kV beam, while it is always deeper, as is shown by the simulations. In Figures 1(g) and 1(h), also shown is the average distribution of deposited energy per ion. In the 5 kV simulation, the total amount of deposited energy was found to contribute in 33% to ionization (loss to target electrons), in 62% to phonons (generation of target atom vibrations), and in 5% to target atom displacements (generation of vacancies, interstitials, and sputtered atoms), creating an average of 144 vacancies per ion, and an average of 1.2 sputtered atoms per ion. In the 30 kV simulation, the total amount of deposited energy was found to contribute in 41% to ionization, in 54% to phonons, and in 5% to target atom displacements, creating an average of 747 vacancies per ion and an average of 2.1 sputtered atoms per ion.

The scrambling of material inside the interaction volume can be utilized for intentional amorphization of crystalline targets or for intermixing layered target materials. Because hundreds of vacancies may be generated by each ion impact, exposure to even relatively small ion doses can result in significant changes in material properties, and as a consequence, fabrication processes that take advantage of such changes may be of high ion sensitivity and fast to perform. In other cases, scrambling is considered a side effect and often referred to as knock-on damage. In certain types of materials, knock-on damage is a serious problem that has to be remedied (see Table 5 for more). Because primary ions get stopped and embedded below the surface of the target material, ion implantation-based applications are possible. FIB-based implantation is rarely used to introduce shallow dopants and alter electronic properties but more often to change general chemical and physical properties. It may be employed for creating a mask pattern in resist polymers or in the target material itself and then followed by an additional processing step that involves chemical or physical etching. The trait that

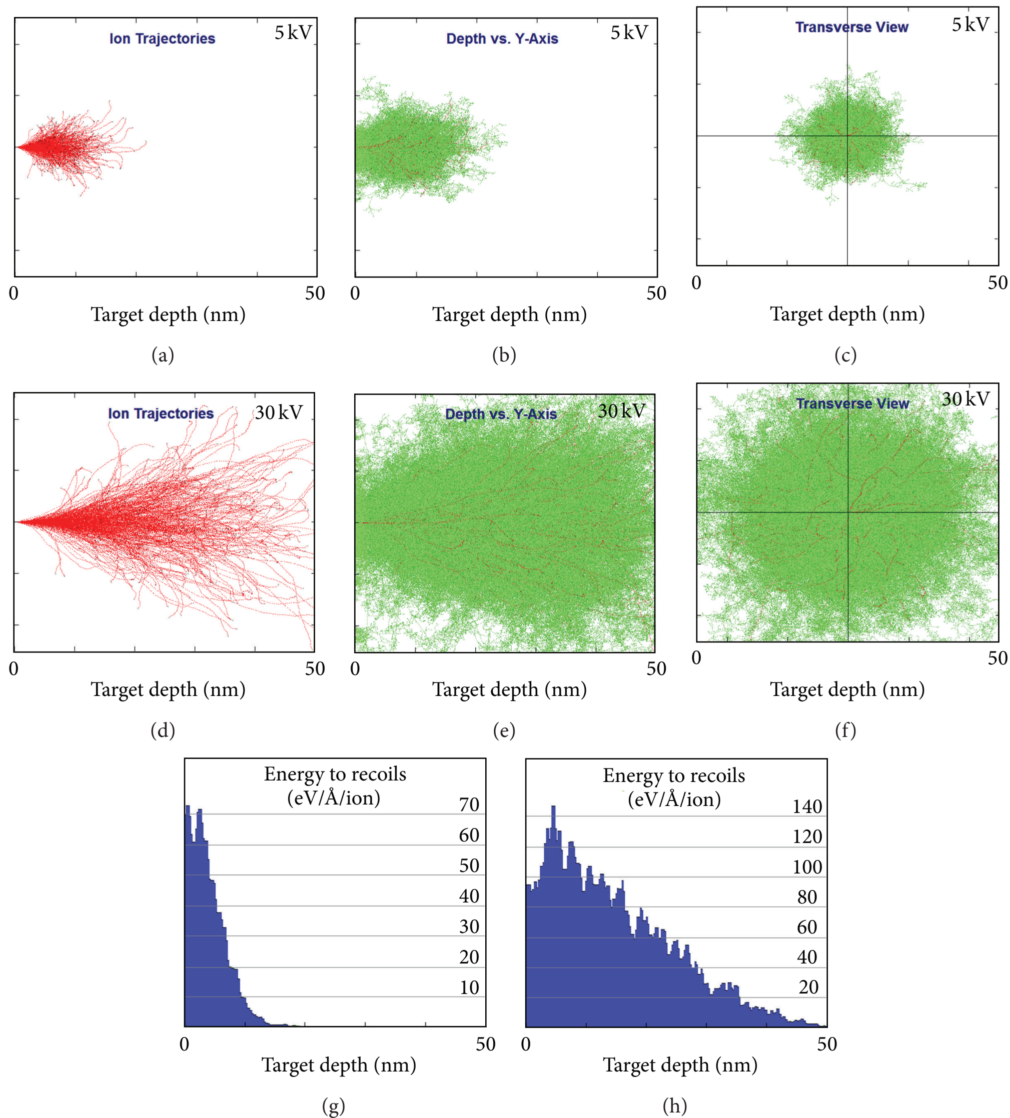

Figure 1: TRIM [4, 5] calculations show simulated collision cascades of 5 kV and 30 kV gallium ions in amorphous silicon (modeled with 2 eV lattice binding energy, 4.7 eV surface binding energy, and 15 eV displacement energy). Plotted are 500 gallium ion trajectories in red, all entering normal to the surface at a single point, each as a single event and then superimposed. The green trajectories are of misplaced silicon atoms, which are plotted on top of the red ones in order to visualize the full volume where changes do happen due to the ion impact. Without taking into account actual gallium ion beam diameters, the simulated interaction volume is roughly 15 nm diameter wide and 15 nm deep for 5 kV and 40 nm diameter wide and 50 nm deep for 30 kV gallium ions. The average distribution of deposited energy per ion is shown in (g) and (h).

ion beam exposure can modify chemical properties is also taken advantage of by surface functionalization applications and by ion-beam-assisted deposition and etching. These latter two use gas phase precursor molecules injected onto the surface of the target material, which would interact with the incoming energetic ions and dissociate. A reactive product can chemically etch the surface, while it is also possible to produce inert species that can pile up and build deposits. Lastly, sputtering of the target material provides presently the most popular use of focused ion beams: direct physical milling. This process usually involves relatively large ion doses, as typical sputtering yields can be relatively low (for gallium ions, yields vary between $10^{-1} < Y < 10^{2}$ [3, 8]). We have summarized the above introduced various types of fabrication processes in Table 1.

3. Focused Ion Beam Instruments for Lithography

FIB instruments are built to serve manufacturing industry and research laboratory needs all over the world. Commercially available machines are specialized and can be roughly categorized as follows.

Table 1: Summary of fabrication processes with focused ion beams and the corresponding physical phenomenon behind them.

Fabrication process	Physical phenomenon behind
Milling	Surface sputtering
Etching	Chemically enhanced milling (directed/localized reactive ion etching)
Deposition	Gas-phase precursor dissociation on the surface (ion-assisted chemical vapor deposition)
Surface functionalization	Creation of surface defects at low ion doses
Intermixing (layered materials)	Destruction of atomic order in interaction volume
Amorphization (crystalline materials)	Destruction of atomic order in interaction volume
Implantation (to alter general physical/chemical properties more often than electronic properties)	Chemical and/or physical change resulting from the incorporation of ions
Resist exposure (a lithography step that requires further processing)	Chemical bond dissociation or formation by interaction with secondary electrons during implantation of organic and inorganic polymers

(1) FIB instruments that are used in industry for a dedicated task such as engraving, semiconductor circuit editing, optical mask repair, or for failure and fabrication process analysis are well equipped and automated for optimum performance.

(2) FIB instruments in R&D are often built on versatile platforms and usually allow a wide range of applications including sample preparation for transmission electron microscopy (TEM) and atom probe tomography (APT) and are mostly equipped for analytical work, such as ion beam tomography, by hosting various detectors. With built-in capabilities or add-on lithography packages, basic patterning and rapid prototyping are possible. Some automated procedures are available, but manual operation is often employed.

(3) FIB instruments in R&D that are geared towards high resolution nanofabrication are built as integrated ion beam lithography systems, providing superior control of beam positioning and navigation on the sample/wafer but little or no analytical capabilities. System architecture, sample stage, electronics, software, and automation are based on a technology similar to dedicated electron beam lithography systems.

All FIB instruments have the following main components: ion source, ion optics (beam focusing, beam shaping, and steering column), sample stage, scan control electronics, software, and sample chamber with additional options. Each of these components has critical features that can be optimized for specific application requirements. The critical features that may be considered for ion beam lithography applications are summarized in Table 2.

Instruments that are optimized for lithography applications have perhaps the strictest requirements for ion source and ion optics performance in terms of high resolution and stability. In order to make processes of many hours or even a few days possible, it is crucial that both beam current stability (defines dose control accuracy) and beam on sample position stability (defines beam placement accuracy) are maintained for extended periods of time. With the purpose of providing the best achievable beam current stability, beam profile, and focus for fine patterning, these machines might sacrifice large current operation all together, so that for nanofabrication, the typical optimized range becomes low to medium beam currents (approximately 1 pA to 1 nA). Given a stable emission point in the ion source and a stable sample stage, the beam steering performance of the ion optics directly defines the pattern placement and dimensional accuracy, which is important within one writing field but especially for multifield patterning (see Section 4 for stitching). The sample stage has to ensure accurate and repeatable relative translation as well as absolute addressing at the nanometer scale that enables blind navigation across larger samples and wafers. This requires a feedback loop controlled laser interferometric stage that would be very challenging to build into a 5 or 6 axes eucentric setup known from analytical FIB instruments, and therefore lithography instruments normally favor a high precision 3 axes stage and perhaps offer add-on solutions to enable additional rotation and tilt for rapid prototyping or process development. The stage concept as well as the sample holder and mounts affect the short- and long-term positional stability via mechanical, thermal, and charge induced drift. Minimizing these effects plus monitoring and correcting the beam-sample position during operation is a necessary complement to the stable and high resolution ion source and optics.

Pattern generation and beam control, as given by electronics and software, include many aspects of the nanopatterning functionality. For the electronics, one has to consider components directly related to the beam steering and pattern definition, and those affecting the general quality of the ion beam. In particular, all high-tension power supplies for the ion source and optics, as well as the scan amplifier and the beam blanking supply, have to be stable and low-noise electronics. These latter two also have to fulfill additional speed requirements in connection with pattern generation. Pattern generator speeds are in the 10 MHz regime, referring to a minimum dwell time on the order of 100 ns or below.

Table 2: Ion beam lithography instrument requirements and options to consider.

Instrument component	Important features, requirements, and options
Ion source and ion optics	Highly bright, small spot ion source Long-term source emission stability and a reasonable lifetime Optics design and lens operation optimized for best focus and optimal beam profile, high on-axis angular intensity at various currents, easily changeable for the smallest features as well as for μm, mm, and perhaps cm sized patterns Accurate beam placement and low distortion beam deflection
Sample stage	Accurate stage translation with nm steps and high repeatability Rotation and tilt for 3D applications and process development Sample size from mm^2 for process development to wafer-scale, supporting mix and match with other lithography techniques Exact absolute position addressing for blind navigation High position stability by sample mounts and stage concept Position monitoring, control, and automatic corrections
Pattern generation electronics and beam control	Suitable patterning electronics speed, buffer memory size, and DAC resolution Stable, low-noise electronics (pattern generator, amplifier, supplies) Fast beam blanking and accurate timing of blanking Available various beam deflection styles and built-in patterns
Software	Offering both intuitive manual and automated, unattended operation Supporting lithography pattern design file formats, like GDSII Handling all basic patterning parameters and advanced features like groups, higher level ordering and repetition, pattern alignments, or automatic corrections (see Section 4 for patterning concepts) Allowing user defined sample coordinate-based navigation Available live feedback and end-point detection techniques
Sample chamber and additional capabilities	Architecture and overall arrangement of stage and column should support the main purpose of the instrument Accommodating samples and wafers of appropriate size Suitable loading mechanisms (possibly through load lock) Gas injectors, detectors, microprobes, and other customization should be installed based on need

Sufficient buffer memory size is required for handling large patterns or dedicated filling algorithms, and typically, a 16 bit or larger digital-analog converter (DAC) resolution is a must to enable small dwell distances in larger writing fields. Beam deflection electronics (including blanking) and filling algorithms on the software side are particularly important to consider. Filling can be done in a directional or shape related manner (e.g., concentric), and in general it is important to minimize the number of fractured subshapes, that is, to fill patterning objects in one go without blanking and to apply repetition with a smart beam blanking strategy. Filling algorithms that follow the outer or inner outline of shapes are especially helpful in achieving smooth and high resolution patterning results and minimal side effects (see detailed discussion in Section 4). Overall, a well-developed lithography software covers a wide range of applications and integrates every aspect of the available processing techniques. For instance, with a typically direct patterning technique like IBL, intuitive and fast prototyping or tests for process development are important on one hand. Here, features like patterning on an acquired image, that is, quickly loading or drawing a pattern onto an ion beam image and executing it, or running live feedback monitors that help with dose estimations or convenient parameter optimization are very useful. On the other hand, the software also needs to support complex, large-area, and repeatable nanopatterning (thus also enabling mix & match with other techniques) for unattended, advanced prototyping and for batch production. Offering nearly full automation, supporting common lithography pattern design file formats like GDSII, and allowing sample-coordinate-based navigation with coordinate systems defined by the user are all very important features, too.

Finally, the chamber concept and various additional components have to be taken into account. For a dedicated IBL instrument, where the ion beam is considered to be the primary means of processing and it is mainly applied to nanofabrication, the most favorable and, in particular, stable arrangement is when a high precision sample stage is running in horizontal and the ion column is mounted over it in vertical orientation. This also supports the handling of larger samples and wafers that can be loaded through a load lock in a cleaner and faster way. Components like gas injection systems, additional detectors (secondary ion detector, multichannel plate detectors, etc.), or micromanipulators and microprobes should be installed as needed, depending on the type of IBL applications supported by the instrument.

To learn more about optimization of instrument properties and especially ion source and ion optics optimization, we recommend the review article “Focused ion beam technology and ultimate applications” by Gierak [9]. General system equipment necessities were also formulated by Tseng in his review article “Recent developments in nanofabrication using focused ion beams” [10]. The need for subnanometer stage positioning accuracy, beam-target movements synchronization, multiple types of end-point detection, and/or *in situ* monitoring capabilities were all emphasized already in this latter article, and these concerns were also included in Table 2. We also recommend the book chapter “Focused ion beam and DualBeam technology applied to nanoprototyping” by Wilhelmi and Mulders [11], which deals with requirements as well as techniques.

There are many ways to describe the performance of a FIB instrument, and there are many procedures to attain such data. It is immensely important to understand that instrument optimizations are not universal improvements to all measures of the performance but are targeted towards certain tasks. Optimizing the shape of the ion beam probe (meaning by both instrument design optimization and by actual operational optimization) is a good example. The ion beam profile (current density distribution) at the sample plane can generally be fitted by the superposition of a narrow and high current Gaussian function, a wider and low current Gaussian function, and an even lower current exponential term [12, 13]. The Gaussians comprise a high intensity central peak, while the exponential term (that is often referred to as the “beam tails”) carries only a small, but for many applications, significant intensity. The beam profile may be tweaked to have suppressed beam tails at the expense of a wider FWHM (which is mostly beneficial for fine patterning) or the other way around: a narrow and intense central peak may be produced accompanied with more extensive tails (which improves imaging resolution and which may also be beneficial for some patterning applications) [7, 14]. Measuring, characterizing, or even specifying the performance (and capabilities) of a lithography instrument thus must reflect the requirements of the main application. Typically, the ultimate performance of a FIB instrument is described by imaging resolution, beam diameter, and fabricated pattern resolution that are always tied to corresponding beam current values (and other conditions). Imaging resolution, that is, the smallest gap between two features that are clearly distinguishable in an acquired image (Airy criterion), and the beam diameter, derived from a line scan across a sharp and steep edge (showing a convolution of beam and edge), are measured likewise to electron beam characterization and, by comparison, the numbers for beam diameter are about 1.4 times larger than those obtained for imaging resolution for the same beam conditions and performance level. Although they are currently routinely used, it is under debate how well these two measurements can be executed in the case of a destructive ion beam. For a discussion about FIB imaging resolution, see Orloff et al. [15].

Pattern resolution, that is, the minimum produced feature size, on the other hand, specifically employs the destructive nature of the ion beam and actually describes the ultimate target of the lithography instrument and application. However, this also implies that pattern resolution, as a measure of performance, carries all aspects of a certain IBL process. It is dependent on how ion-matter interactions are utilized in the application, and as various physical and chemical processes take place in different fabrication processes, a range of different pattern resolution values may be found for the same quality ion beam probe. Pattern resolution is usually larger than the beam diameter due to the expansive interaction volume, but it might also be smaller than the beam diameter if the produced pattern is manipulated by a postprocessing technique such as wet etching of silicon upon low-dose gallium FIB exposure, in which the implanted surface patterns act as an etch mask [16]. Picking a certain sample material over another (if the change is permissible) for the same patterning process can also result in a very different outcome in terms of achievable feature size, although the influence of various material properties (atomic mass, layer or bulk, crystal orientation and composition, conductivity) can usually be addressed by optimization of the patterning parameters and sometimes by introducing additional fabrication steps (see Section 4 for patterning techniques). In summary, the pattern resolution is heavily application dependent, and if it was to describe instrumentation then a well-definable model sample and patterning process should be selected for the measurement, and all sample materials should be carefully specified. It is nevertheless a useful measure of the lithography instrument, because imaging resolution and beam diameter are not suited to unveil enough information about the full beam profile of the ion beam probe that is critically affecting the nanofabrication performance in most applications. The best pattern resolution reportedly accomplished by Ga-based IBL is currently below 5 nm [17], where ultrathin silicon carbide membranes were employed as templates and were milled through. The nanopores achieved this way are fast to produce and are in good quality, because the minimal sputtering needed can happen very efficiently and there is minimal modification (damage) to the membrane, as well as minimal redeposition in front and back sides (note that the beam profile is also not fully reflected in this example of pattern resolution, because the minimal pore size here relies solely and intentionally on the central peak of the current density distribution).

Other specifications measuring instrument performance are system stability and pattern placement accuracy. For system stability, both beam current stability and beam on sample position stability are examined. Measurements are done by frequent read-outs of a Faraday cup (inside the ion column or on the stage) over a period of at least several hours for the beam current investigation, which is affected by the ion source emission and column and electronics stability. For the same time frame the beam on sample position stability test is usually conducted, which is sensitive to the source emission performance, column and electronics stability, stage and sample drift, as well as environmental conditions in general (temperature, vibrations, acoustic noise, pressure). Beam position tests can be based on imaging a reference feature on the sample over time or patterning a large design in many parts that are temporally offset. Typical values for

Table 3: Ion sources (list of LMIS sources from [7, 20, 22, 163]). The ion species listed as "available" are available from well-developed sources and are featured in commercial instruments.

Source type	General properties	Ion species
Liquid metal ion sources	Virtual source size 10–20 nm Typical pattern res 10–20 nm Typical beam currents up to a few nA for Ga and up to 10–100 pA for most other species Very good long-term stability and lifetime for Ga, improving performance for well-known systems like AuSi and AuGe Sputter yield mostly medium to large	Available: Ga, Au, Si, Ge Also exist: Ag, Al, As, B, Be, Bi, C, Ce, Co, Cr, Cs, Cu, Dy, Er, Fe, Hg, In, K, Li, Mg, Mn, Na, Nb, Nd, Ni, P, Pb, Pd, Pr, Pt, Rb, Sb, Sm, Sn, U, Y, Zn
Gas field-ionization sources	Virtual source size below 2 nm (He, Ne) Typical pattern res 5–10 nm Typical beam currents up to 10 pA Limited stability and lifetime Sputter yield mostly small to medium	Available: He, Ne Also exist: H, Ar
Plasma sources	Virtual source size ~10 μm Typical pattern res 100 nm–1 μm Typical beam currents up to a few μA Good stability Sputter yield mostly medium to large	Available: Ar, Xe Also exist: H, He, N, O

Ga FIB, acceptable by most applications, are about a few percent in a few hours and a few 100 nm/h, for beam current and position stability, respectively. Better instrument performance can be achieved by (automatic) drift compensation, which in the case of beam current is based simply on current readings and accordingly applied dose corrections. Beam position compensation is very important for high precision patterning over extended periods of time and on samples with limited conductivity but has to be integrated more carefully into the overall process. This includes selecting the kind and position of a reference feature (sometimes preferred outside the writing field, thus requiring a highly precise sample stage) and finding the "natural breakpoints" of the process flow, for example, at certain points in the pattern execution process, after finishing a writing field or after a specific time. Finally, a good compromise of overall accuracy, time overhead, and homogeneity of final results shall be found. A reference sample with periodic, nm-scale features may be used in measuring pattern placement accuracy (mainly beam placement and deflection accuracy), but a writing field stitching test can also be employed to include stage accuracy in the results. The field stitching test pattern consists of many writing fields with test shapes at the boundaries of each field that are supposed to meet. Afterward a statistical evaluation over this array of writing fields shows the stitching performance, which can be as good as a few 10 nm.

Although most people work with gallium FIBs today, from the applications point of view it would be beneficial to use other ion species in many cases, and so we finish this section with a general discussion of the history and current status of ion sources. There are, indeed, various types of ion sources and a wealth of different ion species, some of which are commercially available, and others that exist in custom built research laboratory setups only, to be used in niche applications or to be further developed. The state of ion source technology is historically an enabling factor for FIB instruments. In the early 1970s, the plasma source of an ion implanter was used for the first time to process maskless samples in the same style as FIB instruments would do today [18]. For an early review of ion sources and instrumentation, see Melngailis [19]. In the next decades, the technology of plasma sources, as well as the developing technology of field-ionization sources, was battling to provide high brightness and small spot size concurrently. Ultimately, liquid metal field-ionization sources (LMIS), and in particular, Ga-based LMIS, matured to be the basis of the modern high resolution FIB instruments. For a short history of ion source technology, see Orloff [20]; to learn about field-ionization sources in detail, see the book of Orloff et al. [7] or a review article by Orloff [14]. For a brief introduction to the Ga-FIB technology, see Volkert and Minor [6], and for an article about Ga-LMIS optimization for nanofabrication see Van Es et al. [21]. While gallium is a material uniquely suited, for best LMIS performance (it is liquid at room temperature and provides a source with adequate stability, a relatively long lifetime, small spot size, and favorable ionization and emission characteristics), there is a list of other ion species available from LMIS (see Table 3) with the use of alloy sources and mass-separation integrated into the ion optics [22]. The range of available species is further enlarged beyond elemental distinction by the presence of different states of charge and mass in which ions (and clusters of ions) may be emitted from a single source [22, 23]. Selecting out certain isotopes and charge states can have peculiar effects on the type and depth of the ion-matter interactions (as well as on the beam diameter). Dependent on the acceleration voltage and the charged particle type (double charged, light ions to heavy clusters) various applications are enabled: from general high resolution work on thin layer samples to fast milling in volume samples, as well as ion specific shallow implantation

and functionalization. Recent developments of certain liquid metal alloy ion sources (LMAIS), such as AuSi and AuGe sources with reasonable stability, lifetime, and easy handling, grant access to ion species of high interest to be built into lithography systems. Nanopatterning applications with much potential include low contamination processing of Si-based devices with Si ions and surface functionalization with Au ions [23, 24].

Another type of field-ionization sources (discovered earlier than LMIS) is based on ionizing molecules adsorbed from their gas phase. These gas field ion sources (GFIS) are in use for producing ion beams of hydrogen and noble gases by condensing them first, followed by electric field-ionization on an atomically sharp needle, this way creating very small (sub-nm) diameter and small current beams. The use of helium ion beams for lithography on resist materials was recently evaluated with high expectation, as helium ion beam lithography is anticipated to outperform both gallium ion beam and electron beam lithography in pattern resolution [25–27]. Neon has also been successfully operated in GFIS, and it shows ultrahigh resolution microscopy as well as nanopatterning capabilities similar to helium [28]. The use of GFIS for lithographic applications is restricted by apparently relative short lifetime and limited stability, in combination with a limited emission and thus small beam currents as produced by the cryogenic source.

Yet another category of sources may be referred to as "volume" sources, which are using gases confined on the μm to mm scale for extracting ions. The ionization can be done by various methods (plasma: [29, 30]; laser-cooled: [31, 32]; electron bombardment: [33]), whereas the use of an electron cyclotron resonance plasma or inductively coupled plasma is the most relevant for the topic of this paper and is therefore included in Table 3. Some commercial FIB instruments feature, for example, xenon plasma sources that are more efficient in milling than gallium beams due to higher sputter yields and larger overall beam currents, which is especially useful for large-volume material removal in certain sample preparation tasks such as in failure analysis applications.

It is beyond the scope of this paper to discuss in more depth all existing and developing ion sources, as it is beyond our possibilities to judge the capabilities of each and every source in general and to evaluate them for nanopatterning requirements. Nevertheless, we would like to give a guideline for such an assessment and point out important aspects to consider for understanding strengths and limits of the source concepts as well as ion species. Regarding the source technology, brightness is an important measure, which includes the source size (partly defining the beam spot size) and the available beam current. Moreover, the stability of the emission and emission control resulting in a certain beam current and beam position stability is, as discussed before, a very important attribute from a nanolithography point of view. On the other hand, the physical and chemical nature of the employed ion specie determines the size of the interaction volume and the accessible processes due to the interaction in general. This determines patterning-relevant characteristics like the beam resolution laterally but also in Z direction (depth), the type of damage to the sample (underneath and outside the pattern), and the milling speed. For instance, light ion species usually can show a good lateral beam resolution but involve a deep interaction volume inside the sample material and can exhibit a sputter yield two orders of magnitude smaller than gallium, which makes milling impractical. Also, the possibly deep implantation can cause serious damage in the sample material even with chemically inert ion species [34]. On the other side of the spectrum, heavy ions (and even clusters) produce a much shallower interaction volume in the sample and show significantly larger sputter yields. However, focusing these beams into a fine spot is more than challenging, and the available minimal spot sizes are thus mostly limited to around 50 nm (this is strongly dependent on the available source too and, e.g., for gold ion beams the minimal spot size can be as small as 10 nm).

4. Ion Beam Lithography Patterning Concepts

Ion beam lithography, the process of producing patterns with an ion beam, is technically very similar to electron beam lithography (EBL), as it uses a highly focused charged particle beam for the purpose of material modification at the surface of a sample, and it uses the combination of beam deflection and target translation for tracing out the desired pattern. Because of this, most already developed EBL patterning techniques directly apply and can be used in IBL. However, in most applications, processing with an ion beam is very different from "simply" exposing a sacrificial resist layer, and therefore there is a clear need for additional control elements. For example, the ion dose cannot simply be converted to a matrix of dwell times and dwell points, each point to be exposed at once, but is usually divided into many portions and delivered in multiple rounds. The order of the dwell points during exposure is also very important. The processing parameters appropriate and necessary for writing with an ion beam, as well as other general IBL patterning concepts, will be investigated in this section.

It is assumed that the FIB instrument is equipped with a digital pattern generator and that the lithography patterns are presented in GDS, GDSII, or a similar format that is conventional for transferring layout designs between different fabrication equipment. Although this is not an absolute requirement for doing IBL, it is definitely a boon. As long as the FIB instrument is prepared to process pattern information in GDS file format, the user can enjoy the flexibility of importing lithography patterns from other tools and can easily build a multilayer fabrication process, where IBL can be an integrated processing step in the workflow. The GDS format is routinely supported by all electron-beam lithography instruments as well. Lithography patterns are composed of the description of patterning objects (sometimes referred as design elements) that are geometric shapes defined on a multi-level hierarchical master plan. Besides the geometric information, lithography patterns carry other information attached to single patterning objects, or attached to groups of objects, or attached to full patterning layers.

Table 4: Basic processing parameters attached to patterning objects and groups of objects and their typical values. Note that the typical values in this table are provided in general to cover various possible operating conditions in the diverse applications of IBL and that individual patterning tasks usually cover much smaller ranges.

Basic parameters of patterning objects	Typical values
Optional use of a gas injector or other assisting device	Yes/no
Ion beam energy (acceleration voltage)	5–50 kV
Ion beam current and beam diameter (spot size)	Smallest is below 1 pA and below 5 nm diameter. Largest is over 1 μA and over 1 μm
Dwell distance (distance between dwell points, also referred to as step size or pitch)	50%–200% of spot size
Dwell time (duration of stay unblanked over a dwell point)	50 ns–1 s
Scan style (order of dwell points inside an object, determined by a filling algorithm and performed by vector scanning)	Line scans or concentric scans are typical, arbitrary paths are possible
Repetition number (objects and groups can be repeatedly scanned, also referred to as loops or passes)	1–10000 for milling 100–1000000 for gas assisted
Wait time (repeatedly scanned objects and groups can have a delay in between scans, also called refresh time)	0-1 ms
Order number (objects and groups are scanned one after another in the order defined by this number.)	Order numbers are assigned automatically if not set manually

The key question now is the nature and the amount of this additional information. In other words, what parameters do we need to attach to patterning objects to be able to sufficiently control the IBL process, and how do we go about designing a lithography pattern like this?

The basic parameters attached to patterning objects and groups of objects are listed in Table 4. Each patterning object in a design can have its own set of basic parameters, and besides the attributes of ion beam manipulation, this set also includes additional switches, such as the indication of using a gas injector or any other assisting device (like an electron flood gun for surface discharging). As a consequence, the various types of IBL fabrication processes (e.g., milling, deposition, and surface functionalization) can all be accommodated in a single lithography pattern. The ion beam energy is chosen appropriately for the desired fabrication process, keeping in mind that lower acceleration voltages will result in a shallower exposure but a somewhat larger beam diameter (spot size) due to poorer ion optics performance. The beam diameter is also affected by the selection of beam current, and this dependency is especially strong with field-ionization sources. Here, the choice of a larger beam current brings about a larger available beam diameter and thus a lower available patterning resolution. Ultimately, high resolution lithography thus must be limited in processing volume (pattern area or depth/height) to keep a reasonable overall processing time. Most lithography patterns can be designed such that the finest features are carried by a small number of patterning objects carefully grouped together and assigned to a small beam, while the bulk of the job is assigned to larger beams, as appropriate.

Patterning objects are comprised of dwell points that are in a regular grid at certain distance apart. The ion beam is scanned over the objects in a user-selected style, visiting all dwell points and stopping at each for the set dwell time. The scan of an object may be repeated several times as set by the repetition number, which results in an overall delivered ion dose of

$$\begin{aligned} \text{Ion dose } & \left[\text{C/cm}^2\right] \\ & = \text{Current } [\text{C/s}] \cdot \text{Dwell time } [\text{s}] \\ & \quad \cdot \text{Repetition } [1] \cdot \left(\frac{1}{\text{Dwell distance } [\text{cm}]}\right)^2. \end{aligned} \tag{1}$$

The concept of repetition is introduced for multiple purposes. In the case of milling, the mill profile is largely affected by the repetition number, and it is critical in cleaning up redeposited material. In ion beam deposition, tiny dwell times are needed to successfully dissociate precursor molecules without sputtering much of the resulting deposits away. The scans in deposition are repeated with a small delay (wait time) in between, or the beam current is selected below a critical current density with respect to the average design element size, which allows for the continuously flowing processing gas to repopulate on the surface. Repetition is also used to lessen charging artifacts by allowing time to dissipate. Last, there is an order number assigned to every patterning object, establishing the order in which the objects are scanned. Setting order numbers and repetition numbers appropriately allows for serial or parallel processing of objects in a group, or even a combination thereof for optimizing both redeposition and resolution. Figure 2 illustrates the effect of filling algorithm and repetition number on milling. In cases where no repetition is applied, the re-deposition of sputtered material is significant and largely alters the mill profile, as

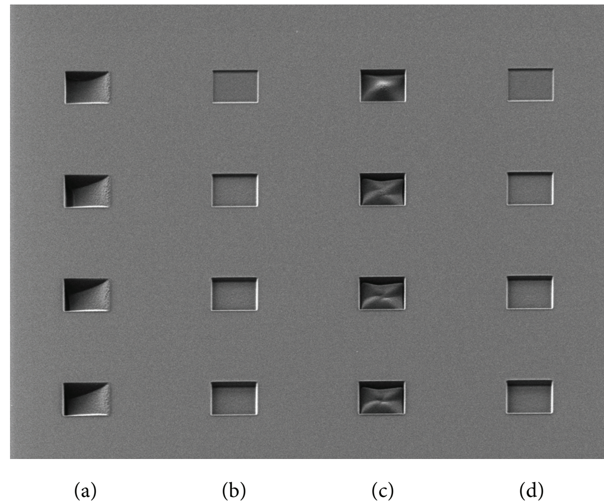

Figure 2: Secondary electron image scanned with gallium ions at 45 degree sample tilt of 1.5 μm size square-shaped patterns milled in single-crystal silicon showcase different filling algorithms and timing. Meandering vertical lines filling from right to left was used in ((a) and (b)), and filling with concentric annular frames from center outward was used in ((c) and (d)). The full dose was delivered in one scan in (a) and (c), while the dose was distributed to 200 repetitions in (b) and (d). The ion dose is increasing downward along the squares by the same amount in all columns ((a)–(d)).

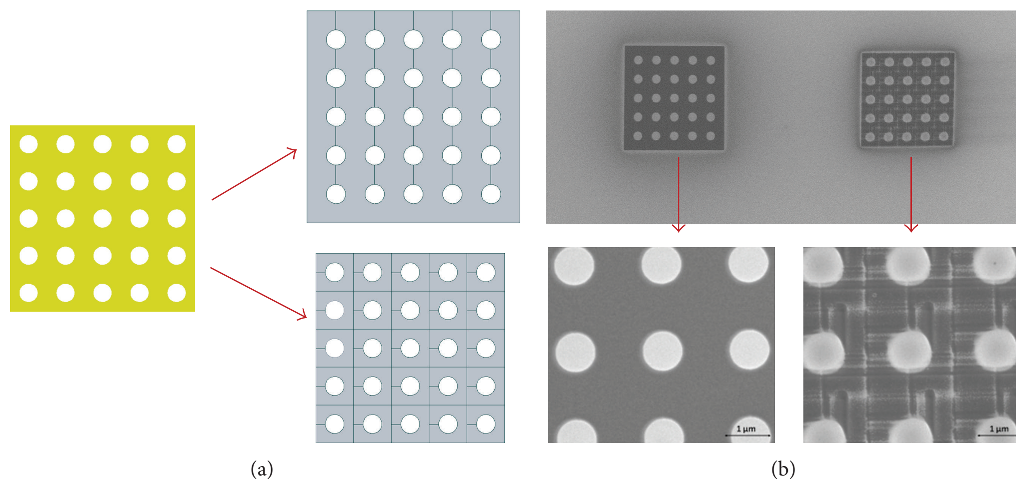

Figure 3: Patterns with unconventional shapes are converted into filled polygons in the GDS description, which can be done in various ways (a). Not only it is important how patterns are defined by patterning objects, but also how those objects are scanned according to the filling algorithm applied. SEM images in (b) show apparently different pattern quality when islands are created using different approaches to fill the space around them (other parameters are the same: 30 kV, 57 pA Ga ions, 1 μs dwell time, 22 nm dwell distance, 500 repetition). The pattern on the right was processed by an e-beam lithography software connected to drive the ion beam, while the pattern on the left was filled by line scans that run intermittently along the whole width of the pattern. The sample material is single crystal silicon with native oxide on the surface.

seen in Figures 2(a) and 2(c). In Figures 2(b) and 2(d), where a suitably large number of repetitions is applied, the mill profile looks similar regardless of the different scan styles. The choice of filling algorithm can be crucial nevertheless in obtaining high quality patterns at the nanoscale, and this is one of the most important differences between IBL and EBL from the lithography software point of view. In Figure 3, we show the task of island milling as a classic example. In the case where e-beam style lithography software was used for processing, the pattern was fractured into several simple shapes that were then filled by line scans, which is a common approach in EBL. As a result, features emerge inside the milled pattern, while the outside of the pattern area is also affected by the increased number of beam blanking that increases unwanted ion exposure of the sample. Blanking lines are traced as the beam is deflected for blanking at the end of a scan. Dependent on the position of the dwell point on which the scan finishes, blanking lines might go across other patterns in the field of view and lightly expose them. It is the best practice to employ filling algorithms that minimize the number of blanking

events. It is also often beneficial if the order of dwell points is such that the scan finishes with the outline of the patterning objects.

While the surface modulation on the mill profile in Figure 3(b) occurred unwanted, it shows that fine 3D features may be produced easily with suitable patterning object definitions and appropriate parameter settings. In general, 3D modulation inside a pattern can be approached by breaking down the complicated geometries to simpler parts and applying on them either dwell time modulation or repetition number modulation.

Besides ion beam parameters, scan styles, and repetition discussed above, there are many other factors contributing to the final quality of patterns. The most blamed hindrances are undesirable features of ion beam profile (width of the Gaussians and intensity of beam tails) and the fact that sputter yield changes with ion beam incidence angle, channeling, charging, and knock-on damage. A list of the most encountered patterning issues along with their causes and possible solutions is given in Table 5.

Writing fields are user selected portions of the ion beam scan field at certain magnifications and are applied as basic area blocks for covering large-area lithography patterns. While executing an IBL process, the ion beam is scanned inside writing fields in a manner determined by the patterning parameters of the lithography objects present in the design. Upon completion of processing a writing field, the stage is translated and the processing of another writing field in the design can begin. The tiles of writing fields can be laid down on the design patterns in various ways, often done automatically using a single writing field size that is chosen based on two considerations. First, the size of the writing field divided by the digital resolution of the patterning electronics (e.g., 16 bit addressing) should be less or equal to the required dwell distance. Second, if larger writing field sizes are permitted by the design, then the size will be limited by the amount of deflection distortions affordable. The larger the area of the writing field is, the more distortions in scanning will occur near the edges. High resolution lithography that requires sub-20 nm pattern placement accuracy throughout the whole design is typically limited to about 100 μm size writing fields (exact numbers depend on the level of optimization of the ion optics for deflection accuracy, and the actual way accuracy is measured and determined, i.e., exact procedure, and definition by mean + sigma or mean + 3 sigma, etc.).

The automated procedure of producing large-area patterns by lining up writing fields on the design and performing stage movements in between them is called stitching. The position of the stage, as well as the positioning of the ion beam, is closely monitored to ensure accurate pattern placement without the need for fiducial markers on the target. For accurate stitching, it is essential that the writing field is well calibrated and aligned with stage movements. This can be done with alignment procedures similar to that in e-beam lithography instruments and can be automated.

The procedure of producing patterns at precise locations by registering to fiducial markers on the target is called pattern overlay. This involves observation and identification of the fiducial markers and matching of their coordinates to those defined in the design by introducing writing field corrections such as shift, stretch, and rotation. Pattern overlay is used primarily in mix & match workflows, when IBL has to be performed on preexisting lithography patterns. In some cases, multistep IBL processing might produce fiducial markers that are used in the following IBL steps. Also, the "relay-style stitching" described in [11] is actually a pattern overlay procedure, where alignment marks are incorporated into the pattern to be read back using overlapping writing fields after every stage movement. In [35], the procedure of pattern overlay on prefabricated, EBL defined markers was found to greatly improve large-area pattern placement accuracy as compared to stitching with the available open-loop stage. However, the fabrication of high resolution fiducial markers in this case required several extra steps, and thus the results highlight the true need for a closed-loop laser-interferometric stage for high-precision stitching.

Even if neighboring writing fields are perfectly stitched, edge effects at the boundaries can show up in those patterns which lay across boundaries, as they are inevitably processed broken by the boundaries. There are four methods to address this issue.

(1) Repetition at the Level of the Entire Multifield Design. Repeat processing the entire design has the same effect on patterns crossing writing field boundaries as common repetition would have on two directly adjacent patterning objects inside a writing field.

(2) Offset Lithography. Offset lithography mitigates the edge effects not just by repeating the entire design, but also by moving the boundaries around with each repetition. This way patterning objects in the design get broken in a certain manner by writing field boundaries for only a portion of the overall received processing ion dose.

(3) Overlapping Writing Fields with Complementary Dose Profiles. This method is based on overlapping neighboring writing fields and dividing the dose for the objects that lay in overlapping regions onto the two fields involved. Division of the processing dose should be done preferably in a smooth and complementary way in order to minimize edge effects. For example, a wedge-like dose distribution can be applied so that the superposition of the two writing field overlaps gives 100% dose throughout.

(4) Continuous Writing Strategies. If the IBL instrument is prepared for this style of "writing field free" operation, patterns may be traced on the target exclusively by stage translation (or nearly exclusively, as ion beam steering might be used for minor corrections, e.g., for the positioning of the start or end point of an object). This allows for continuous patterning of large distances, for example, drawing lines that are several cm long without any kinks. Similar to methods 1 and 2, repetitions on the level of the design or design element should be used (apart from thin layer milling or other low dose exposures), and this is certainly possible with a limited

Table 5: Patterning issues and strategies to deal with them.

Patterning issues	Causes and solutions
Mill profile: rounding of the edges and inclined sidewalls	Caused by the combination of Gaussian beam profile and by the fact that the sputter yield is larger at small angle of incidence (i.e., on sidewalls), and in some cases by re-deposition Edges that are particularly important to be sharp should always be finished last in order and with a small beam current If the beam profile and the scan style cannot be further improved, an additional, sacrificial thin film of material might be coated on the sample, which would take up much of the rounding and that would be removed after IBL patterning In some applications, it may also be useful to consider tilting the sample a couple of degrees from normal incidence in order to produce edges that are vertical to the sample surface
Mill profile: uneven surfaces and poor pattern definition due to differential milling	Caused by the fact that milling rates depend on crystal orientations present in the sample (strongly channeling orientations sputter less) "Thin films of polycrystalline material on an amorphous or single-crystalline substrate are best milled with a small number of passes and a long pixel dwell time The obtainable definition of the pattern will in most cases outweigh the FIB milling artifacts in the substrate due to long dwell times" [11]
Surface roughening/ripple formation	Surface roughening and ripple formation are reported on single crystal targets as well. It is attributed to the competition between the changing sputter yield with angle of incidence (drives roughening at certain patterning parameters set) and surface diffusion (that might help smoothing). See [6] for more on this
Swelling	Swelling is the geometrical consequence of ion incorporation into the sample material and of the destruction of crystalline order. When the ion beam incidence is rather normal to the sample surface, swelling is often observed in early stages of the milling process at low ion doses. Swelling also contributes to the general mill profile by raising up material near the milled edges. See the entry "knock-on damage and incorporation of ions" (below) for prevention and treatment
Mill profile: unsatisfactory depth and/or shape due to redeposition of sputtered material inside pits	Example mill profiles affected by re-deposition, as well as "clean" results achieved by increased number of repetition, are shown in Figure 2. It is important to note that as the aspect ratio (depth to width ratio) of a milled pattern is increased, it becomes less and less frequent that the sputtered material is projected out of the hole or trench during milling. At around 10 : 1 aspect ratio, the milling effectively stops regardless of scan style or repetition number It is possible to increase aspect ratios (as well as to speed up the milling process) by gas-assisted etching. When a chemically reactive gas is introduced at the site of patterning, the milling can be enhanced due to gas-phase reaction products that escape from the high aspect ratio patterns. Using reactive ion etching will change the mill profile in other ways too, dependent on actual chemistry, pressure/flow rate, ion energy, and so forth
Re-deposition	In general, re-deposition of sputtered material is a difficult issue with complicated, large volume, or 3D designs, especially if the milled pattern is physically enclosed in its location, or if closely surrounded by other lithography features In most cases it is feasible to finish milling with the outline of the finest (or most sensitive) structure, polishing up with small beam currents. Moreover, the use of an etching gas increases the volatility of the removed material and can help to minimize re-deposition
Charging and positional drift	If the sample is electrically insulating or involves smaller size electrically isolated islands, charges will not be able to dissipate at the site of patterning. Charging can cause drifts while accumulating; melting and explosions can occur during discharge. Charging may be prevented by applying one or more of the following: coating the surface with a conductive thin film, assisting opposite charges with an electron gun, or assisting a nonreactive gas locally (that could be water vapor dependent on the target material). Automated drift correction, in which a fiducial marker (reference point) is visited periodically for detecting and correcting shift in positioning, should take care of minimal charging issues and instrument positional drift in general. Also see [135, 164, 165]

Table 5: Continued.

Patterning issues	Causes and solutions
Knock-on damage and the incorporation of ions into the sample	The unavoidable but limitable and sometimes curable side effect of ion beam processing is the undesired change of atomic order in the interaction volume. In particular at higher beam energies, the collision cascade can reach deeper and wider (see Figure 1 for a reference in silicon) There are four aspects of dealing with knock-on-damage. (1) The damage can be directly reduced by reducing the ion beam energy. This is exactly why low kV polishing is commonly employed as a last step in TEM or APT sample preparation (2) The damage may be recovered by treating the sample after IBL. Annealing is often reported as a successful means to heal crystal defects or recrystallize, and sometimes it is possible to expel the incorporated ion specie content (3) In general, the damage can be minimized by scanning only outer parts of the sample and the reference or alignment marks and using "blind" navigation and pattern placement. Then just the processing dose itself is applied to the crucial or sensitive parts of the sample (4) Part of the processing dose damage is also avoidable. Unintended ion exposure from beam tails and from ion blanking lines may be blocked by coating a protective thin film on the surface (for hard masking). The protective coat may be removed later easily, if its material is chosen suitably and is compatible with the sample material Note that crystalline samples might go through amorphization, alloy phase formation, and/or ion beam induced grain growth. See also [3]. Also note that these changes can be beneficial and be taken advantage of in some nanofabrication processes. Examples are listed and discussed in Section 5
Shadowing on surfaces and curtaining effect on cross-section cuts	Uneven topography in the line of sight of ions causes shadowing and curtaining. Even if the original surface is flat, uneven topography can develop if the sample exhibits differential milling, and/or if it is composed of various materials of different sputter yield. See also [3]
Deterioration of fiducial markers	Caused by unintended milling of the fiducial markers during observational scans. Fiducial markers (also referred to as alignment marks) mark specific locations on the sample to be used for drift correction, pattern overlay, and write-field alignment. Fiducial markers may be produced by various methods (dependent on the place of IBL in the work flow). Besides depositing hard-to-sputter, small grain, or amorphous and conductive materials to fabricate fine resolution alignment patterns, topographical markers should be considered that can be deep etched into the sample, sometimes even by the IBL instrument itself. Markers may be scanned over hundreds of times and sometimes with relatively large ion beam currents (whatever is used for the IBL processing step), so they have to be durable enough to serve as needed. In addition, the concept of a "dynamic mark reference" can be employed, in which the reference image is repeatedly redefined in order to account for changes in shape and size (i.e., after a few mark scans a freshly acquired scan image is saved as the new reference and used for the following alignment procedures)

number of loops applied to the sample stage. More advanced strategies even combine classical beam deflection and specific stage movement for creating patterns other than lines and paths. In particular in this case of complex interaction, synchronization of beam and stage control is crucial and can be done similarly to the write-on-the-fly techniques known from electron beam lithography.

5. Ion Beam Lithography Applications Examples

In this section, different types of structures and patterning tasks are introduced as applications examples of IBL-based micro- and nanofabrication. There are two distinct advantages that IBL techniques can deliver to an application:

(1) simplified fabrication including reduced number of processing steps, while alternative standard patterning techniques usually do exist,

(2) special patterning capability or an enabling technology.

The advantage of simplified fabrication is mostly provided by the high resolution direct milling, etching, and deposition capabilities of IBL. Opting for one of these processes can replace a combination of standard fabrication steps, such as a mask-patterning lithography step, perhaps a mask-material deposition or etch step (if the resist layer itself cannot serve as a mask), and the etching or deposition of the functional material. For a review on milling, see Tseng [36], and for a review on gas-assisted etching and deposition, see Utke et al.

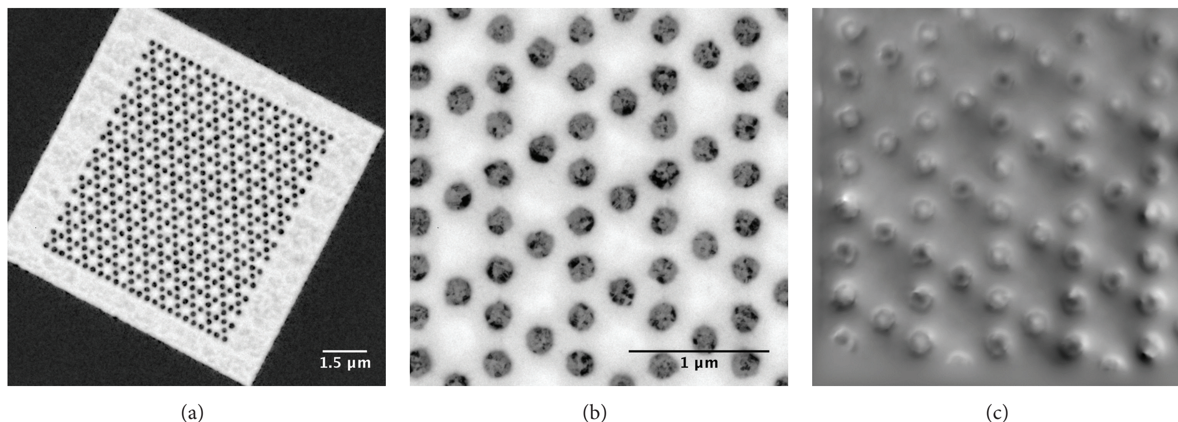

(a) (b) (c)

Figure 4: Bright field TEM images of magnetic islands milled out of a thin film using raster style scanning (pattern was defined by a bitmap image of the design) ((a) and (b)), and their corresponding phase shift image (c) reconstructed by using transport-of-intensity technique shows the islands supporting magnetic vortex states. The dark and bright spots at the center of the islands relate to clockwise/counterclockwise rotation of magnetization. From Ch. Phatak, Argonne National Laboratory, Materials Science Division, presented at the 54th EIPBN conference, 2010.

[37]. For a comparison of IBL techniques with conventional fabrication methods, see Langford [38]. In the case of small batch fabrication needs (applies to most R&D efforts) and even of large batch needs provided that the amount of material to be removed or added is relatively little per device (e.g., magnetic read-write heads, see under *Applications in industry*), IBL can save time, effort, and equipment. In addition, the initial process development effort is also usually easier and faster, because of the rapid evaluations that can be done on the prototype samples inside the IBL instrument. Applications examples of simplified fabrication in R&D are of MEMS devices, magnetic structures, plasmonic and photonic structures, and zone plates. Again, for these types of small-scale sample production, IBL can save time and effort by simplifying the fabrication process, because the same high quality structures would be impossible to reproduce by other methods in such a short workflow. The techniques of IC failure analysis, circuit edit, and optical mask repair as well as sample preparation techniques for TEM and APT also benefit from a significantly simplified sample fabrication, performing multiple processing needs in the same FIB instrument while heavily utilizing a multitude of FIB capabilities. Finally, there are also examples for simplified fabrication, where an IBL technique does not necessarily replace multiple other fabrication steps but does provide a simplified/improved step for the one it does replace. Techniques like this include hard masking by implantation or ion beam lithography on resists.

The advantage of a special capability or an enabling technology is given when a fabrication task is uniquely suited for IBL processing. This may happen by applying the high resolution, direct nature of IBL to special samples or tasks, such as in the case of true 3D deposition and milling techniques (e.g., 3D template fabrication and microfluidic devices), patterning of some thin films for which no other nanofabrication technique is yet developed (e.g., some complex oxides and superconductors), direct patterning tasks on ultra-thin membranes (e.g., nanopores fabrication), and direct patterning tasks on samples with highly topographic features (e.g., scanning probes and microtools). Direct patterning ability on thin membranes, for example, is particularly useful in the biosciences and in materials sciences, where membranes are employed in a variety of sizes and materials. Postfabrication on released membrane windows is usually tricky, especially wet processing or spin coating can be difficult, for which FIB techniques offer an interesting alternative. In particular, the direct milling of nanopores, down to sub-10 nm diameter, is shown to be an adequately controllable process that produces high quality patterns reasonably fast [17, 39]. Another example, illustrated in Figure 4, is the direct milling of thin films coated on membranes. In this case, a sandwich of chromium (2 nm), permalloy (20 nm), and chromium (2 nm) was patterned into a lattice of islands on a merely 50 nm thick silicon-nitride membrane for Lorentz TEM observation of the magnetic behavior. The membrane was somewhat thinned as overmilling was necessary due to differential milling occurring in the polycrystalline magnetic film but was left in good condition and served well during the many TEM experiments.

As mentioned earlier, a group of applications employs IBL milling as a high resolution physical etch method for materials that are difficult to pattern otherwise. Chemical etching or chemically enhanced physical etching (i.e., reactive ion etching) is in general not appropriate for most complex oxides and some metal alloys of high interest (besides other materials). Although these materials might also be processed by broad beam ion milling through a hard mask, this can usually be done only with certain precautions such as the cooling of the samples during milling and/or very challenging masking needs. Such patterning tasks include nanostructuring certain dielectrics for photonics, ferroelectric thin films, and many superconducting materials.

New technologies emerge when unconventional IBL techniques, such as intermixing, amorphization, implantation, or surface functionalization (as defined in Table 1), are employed and new methods are developed with them (see nucleation sites, amorphization, and graphitization of diamond, hard masking, semiconductor processing, and magnetic thin films on the following pages). Take the patterning of ferromagnetic ultrathin films and multilayer thin films with perpendicular anisotropy as an example. Here, patterning is possible at low ion doses, without a significant amount of milling, by simply mixing up the layer interfaces. In fact, as intermixing increases with increasing ion doses, the irradiated films are found to gradually lose their magnetic coercivity and anisotropy and become paramagnetic. This allows for novel design rules in case of closely spaced islands, like the dots for magnetic recording media, where dot-to-dot coupling may be varied in a controlled way from pure exchange to pure dipolar [40]. Because the ion doses required for the above described mixing-based patterning are much lower than that for milling, these thin films can be patterned relatively quickly. It can also be an advantage that the planarity of the sample surface is maintained [41].

In the rest of this paper, our intention is to provide an overview of most pursued IBL fields of applications. Starting with general applications and patterning techniques, the list becomes more specific about various fields of applications and finishes with a link to "patterning for analytical purposes" and an overview of micromachining and applications in industry.

5.1. Nucleation Sites for Directed Self-Assembly (DSA). Defects at surfaces, whether created specifically by low ion dose point exposures or as a result of a deliberate topography milling process, can act as preferential sites for nucleation and growth. FIB-based template patterning for DSA is an increasingly recognized lithography method, as more and more material systems are explored. The templating process itself (i.e., the nucleation or trapping mechanism) can take various forms. For example, ultralow dose implantation of 25 kV Ga^+ ions into Si(100) followed by annealing and molecular beam epitaxy (MBE) of germanium was used to fabricate Ge quantum dots (QDs) by Hull et al. [42], and the location of QDs was found to be in strong correlation with the IBL pattern if the annealing conditions were selected carefully in relation to the evolving surface morphology. Other types of QDs, such as InAs and InP on GaAs substrate, and Cu_2O on $SrTiO_3$ were also produced by other groups. Another set of studies focused on FIB-generated defects on graphite surface, in particular on highly oriented pyrolytic graphite (HOPG) [43], which was found to efficiently trap deposited nanoparticles by dangling bonds [44]. Gold nanoparticles [45], as well as CoPt clusters [46], were templated by this method.

IBL may also deliver ions that themselves form the basis of nucleation. In particular, gold FIBs are interesting for enabling direct patterning of catalyst (where implantation of the gold ions is followed by thermal annealing to form active clusters on the surface of the substrate). For example, laterally growing Ge nanowires were synthesized catalytically using MBE upon annealing gold ion implanted silicon wafers by Marcus et al. [47]. Vertically growing epitaxial GaAs nanowires were produced on GaAs wafer by Gierak et al. [24].

5.2. Amorphization and Graphitization of Diamond and Carbonaceous Materials. Ion implantation into single crystal diamond causes defects by breaking sp3 bonds, which leads to amorphization in the implanted volume. It was found that a critical implantation dose exists at which the diamond lattice cannot be restored anymore by annealing, and instead, a stable graphitic region forms with sp2 bonds [48]. Buried graphitic layers produced by high-dose implantation of several hundred keV or MeV and subsequent annealing are the basis of a so-called diamond lift-off process, in which the graphitic layer is etched selectively by a wet acidic solution or by heating in oxygen environment [49]. Free-standing 3D structures may be produced by this method for MEMS and photonics applications [50, 51]. Low-energy, 30 keV Ga FIB implantation has also been experimentally investigated by Rubanov and Suvorova [52] and the formation of an approximately 35 nm thick amorphous layer was observed in synthetic diamond (001) samples at ion doses that provided complete amorphization up to the surface. Studying a wider range of ion doses, McKenzie et al. [53] reached a similar conclusion. The conductivity of completely amorphized (and later graphitized), approximately 100 nm wide wires on diamond was studied by Zaitsev [54] who observed conductivities higher than the conductivity of bulk graphite and comparable with the conductivity of metals. Changes in refractive index due to lower dose 30 keV Ga implantation were studied by Draganski et al. [55] in order to explore uses in optical device fabrication. While the FIB technique of diamond amorphization and graphitization (including that of nanocrystalline diamond, ultrananocrystalline diamond, and diamond-like carbon materials) is only recently being investigated in detail by the scientific community, it is worth mentioning that the technique has already found earlier application, as there are several patents between 1998 and 2003 describing low-energy and low-dose Ga FIB-based marking of diamond gemstones for producing inscriptions for trackability and other engravings.

Another important point to make is that the technique holds for many carbonaceous materials, including carbides such as silicon carbide (SiC). For example, low-energy (30–60 keV) focused ion beams of Au, Cu, Ge, and Si have been used to produce nanoscale patterns of few layer graphene (FLG) structures on SiC by Tongay et al. [56] and Lemaitre [57].

5.3. Lithography on Resists. Resist-based lithography uses organic and inorganic polymer films as sacrificial layers (usually spin-coated) that undergo chemical bond dissociation or formation due to interaction with secondary electrons in case of exposure to a particle beam (or with photons in case of optical lithography). The chemically altered regions are then

developed in a wet solution. Because the process involves secondary electrons regardless of whether the focused particle beam is of electrons or ions, the resist materials, solvents, and developer solutions are the same for EBL and IBL. In general, ion beam based resist exposure is pursued because

(1) ion beams generate secondary electrons much more efficiently than electron beams; thus the required ion dose is much smaller than the required electron dose, which can make the exposure process much faster (if the same beam currents are available with appropriate beam diameter);

(2) proximity effects are not an issue, as the backscattering is minimal, which makes nanoscale pattern design much simpler.

The limitations of IBL compared to EBL lie in the practical resist thicknesses that can be processed. The heavier the ions are, the shallower the interaction volume is, and, for example, the resist thickness is limited to a maximum of about 50 nm in case of 30 kV gallium ions. A pattern resolution below 10 nm has been demonstrated with gallium ions in poly(methylmethacrylate) (PMMA) by Kubena et al. [58] and in hydrogen silsesquioxane (HSQ) by Bruchhaus et al. [59]. Lighter ions than Ga^+ are interesting because thicker resist layers can be exposed and because they could provide potentially higher pattern resolution [25, 27]. Several ion species are compared by Matsui et al. [60]. Helium ion beams [25, 26] as well as neon ion beams [28] have recently been investigated. Another way to effectively increase resist thickness while using heavier ions is to move away from traditional resist exposure and take advantage of ion implantation effects that can produce a negative resist pattern if developed by reactive ion etching [61–63]. This is a type of direct "hard mask" patterning technique that we discuss next.

5.4. Hard Masking. In the case of certain combinations of sample materials and ion species, masks may be produced directly by shallow implanting the surface with the ion beam. Because the exposed regions are chemically altered by the implantation, the patterns produced can hold up against some chemical etchants that normally attack the sample material and can serve as mask in wet etching [16, 64] or in reactive ion etching [65, 66] processes. Examples include gallium ion implantation of silicon wafers (see prior four references), as well as of single crystal diamond [67, 68], silicon nitride layers deposited by low-pressure chemical vapor deposition, and germanium selenide layers deposited by thermal evaporation [69, 70], aluminum doped zinc oxide, and tantalum layers [2], as well as spin-coated photoresist layers by Arshak et al. [61–63] as was mentioned earlier.

5.5. 3D Template Fabrication. FIB milling is presently the only nanofabrication method capable of producing intricate and high resolution, three-dimensional surface patterns in any solid material, which is especially interesting for templating applications with nanoscale features. Other directly topographic fabrication methods are microtool-based or laser-based. While the process of laser ablation has been investigated at the nanoscale in the near-field of preexisting nanoscale structures [71], controllable and precise ablation-based fabrication is only available at the microscale. Another laser-based 3D fabrication involves direct laser writing in photosensitive materials. Practically any arbitrary 3D photoresist structure may be produced by two-photon polymerization, and this is particularly interesting in the making of photonic crystal structures [72]. However, this method also lacks the resolution needed for nanopatterning in general [73].

Current efforts in 3D template fabrication and usage are as follows.

(1) The seamless combination of different fabrication techniques for 3D shaping at large and small length scales on a template is being explored. In the work of Palacios et al. [74], IBL was combined with photolithography and dry and wet etching to remove larger volumes before fine patterning with a FIB. In another example by Lalev et al. [75], IBL was combined with laser ablation.

(2) In molding with polymers on a 3D template, volumetric shrinkage during the curing process tends to become an issue, altering the imprinted polymer features. See Kettle et al. [76] for more on this, as applied to "motheye lenses" with 9 μm/80 nm lens diameters.

Note that besides FIB milling, FIB deposition might also be used to produce or alter templates. In addition, FIB lithography on resist may be used to produce 3D surfaces in certain polymers [77]. Also note that 2D templates (i.e., those fabricated by milling to a uniform depth or by regular ion beam lithography on resist) are also pursued in some cases, for example, for nanoimprint [27].

5.6. Nanopores and Other Membrane Devices. Nanopores for bioanalytical applications are an exciting field of research which has seen rapid development over the last ten plus years [78]. Membrane-based solid-state nanopore devices for molecule analysis (DNA sequencing) or other biological sensing and filtering applications are widely discussed and used. For a review of solid-state nanopore technologies, see [79–81]. Ion beam lithography is among the most promising patterning techniques to date, capable of providing sub-10 nm pore size and good reproducibility at wafer-scale with little contamination. IBL may be used with various types of membranes, although in general, dielectric materials such as silicon dioxide or silicon nitride are preferred with a thickness of 20–100 nm. IBL milled nanopores have been demonstrated to work in various experiments; see, for example, Japrung et al. [82].

5.7. Semiconductor Processing. FIB implantation may be used for tailoring dopant profiles in semiconductor devices and improve device performance (e.g., [83, 84]. Work on this has been rather extensive and was reviewed by Melngailis in 1987 [19] and also by Langford et al. in 2007 [85]. In an utterly enthusiastic FIB effort, fully FIB-fabricated junction field

effect transistors (FET) were demonstrated [86]. For ultimate doping, single ion implantation has been developed based on a FIB setup for creating custom dopant distributions with approximately 60 nm placement precision with 60 kV doubly charged Si ions, and as a result, studies of ordered dopant arrays were reported [87, 88]. Single ion implantation and its applications for FETs and quantum devices were reviewed recently [89, 90]. In another specialized doping scheme, FIBs are applied for the lateral patterning of two-dimensional electron gases in heterostructures [91].

Besides dopant implantation, another technique for semiconductor processing is FIB implantation induced intermixing (upon thermal annealing) of superlattices. Impurity induced layer disordering allows for altering effective band gap and refractive index in desired regions of quantum well heterostructures, which finds immediate application in optoelectronic devices [92–96]. Both dopant implantation and intermixing techniques work with low ion doses and therefore with very reasonable IBL processing times.

5.8. Complex Oxides. "Complex oxides have many promising attributes, including wide band gaps for high temperature semiconductors, ion conducting electrolytes in fuel cells, ferroelectricity and ferromagnetism. Bulk and thin film oxides can be readily manufactured and tested, however these physically hard and chemically inert materials cannot be nanofabricated by direct application of conventional methods. In order to study these materials at the nanoscale there must first be simple and effective means to achieve the desired structures," wrote Waller et al. [97].

Indeed, one of the main hurdles for the application of nanostructured complex oxides is the lack of developed nanofabrication techniques. The two trends in the nanopatterning of perovskites, the most interesting complex oxides, were reviewed by Vrejoiu et al. [98]. In one approach, nanostructures are grown epitaxially into some sort of a template, and in the other approach, high quality thin films are etched physically, for instance, by IBL. However, when FIB milling is used to produce complex oxide nanostructures, it is critical to introduce measures for damage prevention and for crystal recovery (see knock-on damage and ion incorporation in Table 5, and Klug et al. [99] for a patterning example of ferroelectric $BiFeO_3$ thin films).

5.9. Superconductive Structures. FIB milling is popular in the research of type II superconducting thin films for the physical patterning of superconducting device geometries, but also for the introduction of defects, especially "columnar defects" that can interfere with the breakdown mechanism and push the critical current density of the material higher. The artificial defects, introduced by FIB milling and mixing, work by pinning of the magnetic flux that enter the material during superconducting current flow. Closely spaced, regular arrays of point dwellings are usually employed to collectively pin the naturally emerging vortex lattice (e.g., [100, 101]). In addition to milling-based patterning, it was found that gallium ion beam assisted deposition from tungsten carboxyl gas produces deposits that are superconductive, and wires 300 nm wide, 120 nm thick, and 10 micron long exhibit a critical temperature of 5.2 K. (work done by Sadki et al. [102]).

5.10. Magnetic Structures. Ferromagnetic nanostructures including nanomagnets have many existing and potential applications, primarily in information storage technologies and in relation to biosciences. Patterned media, magnetic random access memories, spin electronic devices, and developing magnetic logic and magnetooptical devices are the main examples of lithographically produced structures. The top-down fabrication techniques capable of producing patterned magnetic nanostructures were reviewed by Lodder [103], and especially FIB-based fabrication was reviewed by Khizroev and Litvinov [104]. The latter article points out that although IBL technology is mostly limited to rapid prototyping (i.e., R&D) type of applications in industry, it is a strongly beneficial choice in this role. And just as in industry, academia and research institutions also gladly employ IBL to fashion magnetic sample materials. While milling is the most popular technique used, there are other interesting processes available, like ion beam induced deposition (of cobalt [105, 106] and of FePt and CoPt [107]) or the intermixing-based patterning of magnetic multilayer thin films [40, 41] that was discussed earlier in this section. For an extensive review of magnetic materials patterning through ion irradiation, see Fassbender and McCord [108].

5.11. Plasmonic Structures. Surface plasmons are electron plasma oscillations coupled to electromagnetic waves and are bound to the interface of an appropriate conductor and a dielectric material. It is their feature of concentration and confinement of energy into nanoscale volumes precisely at the interface which makes them so attractive. Because plasmonics is a surface phenomenon, the structures of primary interest are finely patterned thin films and chemically synthesized nanoparticles. The most used conductor materials are silver and gold for wavelengths in the visible and near infrared spectral range. For more information about plasmonic materials see Blaber et al. [109]. Plasmonics research is still on the rise since the 1990s and while expanding, it has broken into several subtopics that are themselves vast and are reviewed separately. For an earlier review of the whole field see Barnes et al. [110, 111]. Plasmonic structures are currently being developed for embedding into optoelectronic interconnects, high efficiency LEDs, photovoltaics, and sensitive chemical-biological detectors and are applied in medicine.

The nanofabrication of plasmonic structures was recently reviewed by Fu et al. [112]. Besides other popular lithography methods such as e-beam lithography, laser interference lithography, and the less-used nanosphere lithography (all followed by lift-off), IBL is a very widely used technique due to the convenience of creating grooves, cuts, holes, dimples, and small gaps directly by milling. These simple features in the thin films can assist with the generation, propagation and manipulation of surface plasmons. To view examples of FIB milled structures for surface plasmon polaritons see Bahns et al. [113] and for resonant plasmons Rosa et al. [114], the latter also depicted in Figure 5 showing four-segment

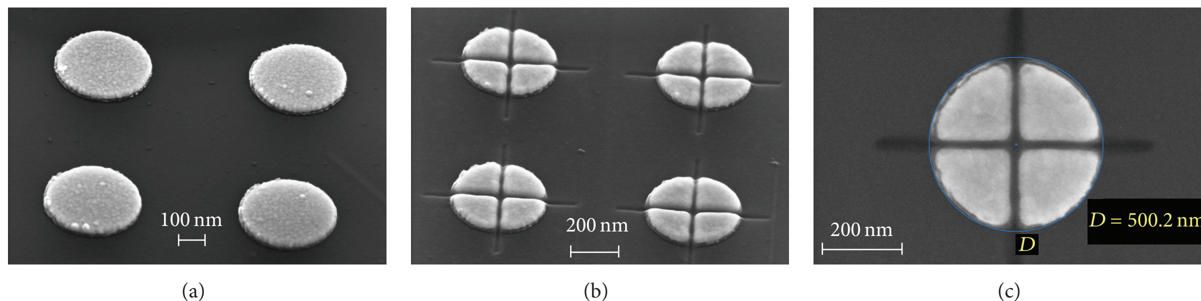

Figure 5: Tilted view (a-b) and plane view (c) SEM micrographs of 40 nm thick segmented gold islands made by overlaid milling of crossing lines. Localized surface plasmons interact through the approximately 20 nm wide gaps that were intentionally overmilled deeper into the silicon, as this feature was predicted to favorably affect electromagnetic field enhancement between the gold segments in the near infrared spectral range [114].

plasmon resonators produced by the combination of EBL, gold evaporation, lift-off, and IBL milling.

5.12. Photonics (Integrated Optics). Bragg reflectors, optical fiber sensors, photonic crystals for vertical cavity surface emitting lasers (VCSEL), one-dimensional and two-dimensional photonic crystal defect cavities, and waveguides are often fabricated by FIB milling and etching in various materials (see, e.g., [115–123]). Three-dimensional photonic crystals, FIB-milled from surface side at two different angles, were fabricated in crystalline TiO_2 by Juodkazis et al. [124]. Microlens arrays have been fabricated by Fu et al. [125] among other groups. Photonic structures have also been fabricated recently in diamond membranes and beams [126, 127], and FIB has been used to facilitate the formation of color centers in diamond, which provide a promising platform for quantum information processing. For a review of diamond integrated quantum photonics, see [128].

Samples usually require treatment for crystal damage recovery and for implanted material removal, which often involve thermal annealing, sometimes selective wet etching, and the use of protective coatings during milling. See Tao et al. [129] for more about postfabrication treatments.

End-face milling for polishing the interface of channel waveguides is widely used. A silicon-on-insulator grating fiber coupler has been demonstrated by Schrauwen et al. [130] and fiber to waveguide coupling by a lens at the end of the fiber is demonstrated by Schiappelli et al. [131]. The modification of optical fibers for sensor application (other than proximal probe) has also been recently investigated [132, 133].

5.13. Zone Plates. Fresnel zone plates are circular diffraction gratings used to focus light (or other waves). They are widely applied in X-ray optics, where the use of traditional refractive lenses is not feasible. For the zone plate's concentric circular grating, opaque and transparent materials are alternated such that the width of the rings decreases as the radius increases. When light passes through the rings, it is diffracted on the opaque regions. The plate is designed to allow constructive interference to occur at a chosen focus point, at a certain distance from the plate.

FIB-based fabrication of zone plates is attractive for the following reasons.

(1) IBL milling is a straightforward, single step fabrication process done directly on the absorbing material, as compared to the multiple steps of EBL templated RIE and electroplating.

(2) IBL can be done directly on membranes instead of wafers or bulkier substrates, again saving processing steps.

(3) For a larger variety of X-ray optics applications there is a demand for fabricating diffracting elements from different materials. Developing the fabrication process with IBL is easier and faster as compared to the other methods.

(4) Patterning of zone plates with a 3-dimensional profile enables higher order focusing and thus a spatial resolution that is better than the expected Rayleigh resolution [134].

The limitation of IBL based fabrication of zone plates is found in the need for high aspect ratio structures. The highest aspect ratio structure of a Fresnel zone plate is the outermost ring, and it has the aspect ratio of the plate thickness over its width. A plate's thickness is chosen for optimal efficiency and the width of the outermost ring is chosen for optimal resolution at a given X-ray energy. Considering the limitation of the producible aspect ratio, it follows that IBL applies primarily to the fabrication of soft X-ray zone plates, where both appropriate efficiency and high resolution can be provided. For example, a 100 nm imaging resolution Fresnel zone plate was demonstrated by Nadzeyka et al. [135], as shown in Figure 6. The 100 μm diameter zone plate was produced in a 500 nm thick, sputter-deposited gold layer, on a 500 nm thick Si_3N_4 membrane, in a 15 hour-long milling process. For another example, see Ilinski et al. [136].

5.14. Microfluidic Devices. Microfluidics is an interdisciplinary field that deals with the physical behavior and the manipulation of flows confined to the micrometer scale and below. Microfluidic devices have had a considerable impact

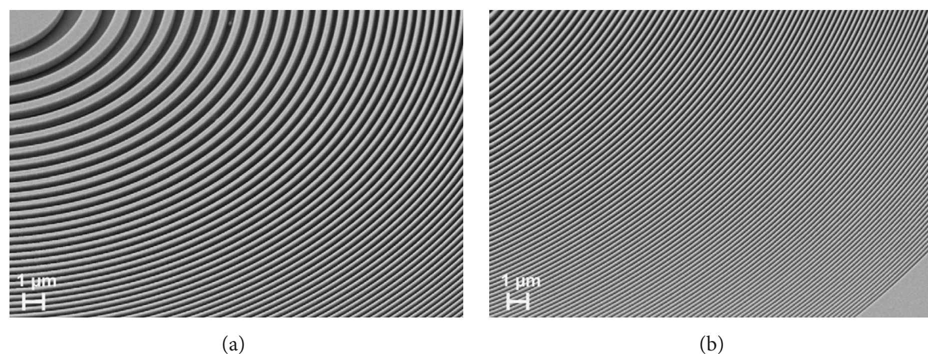

(a) (b)

Figure 6: SEM images of sections of a 100 μm diameter Fresnel zone plate made of gold and patterned by IBL. The outermost ring is approximately 100 nm wide and has a 5 : 1 aspect ratio. This plate was tested and shown to provide 100 nm imaging resolution when used with 1200 eV X-rays. Reprinted from [135].

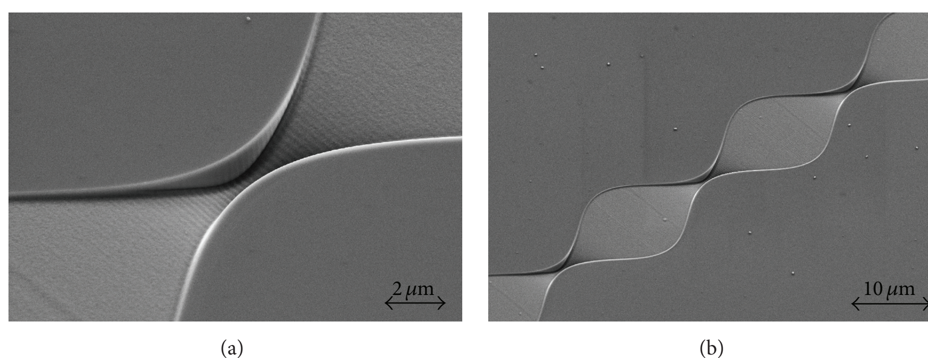

(a) (b)

Figure 7: SEM micrographs at 45° viewing angle of a finely designed three-dimensional microfluidic mixer channel milled by using advanced dwell time control linked with the object filling algorithm applied to the pattern. Reprinted from [74]. The ability to create intricate 3D structures either by milling or deposition is perhaps the most recognized unique feature of IBL. In this example, the IBL-based fabrication of microfluidic mixer devices allows for sophisticated three-dimensional channel geometries that can be fabricated only by direct-write IBL.

on the fields of biomedical diagnostics and drug development and are extensively applied in the food and chemical industries [137]. In all applications, the task of microfluidic mixing has been understood as one of the most fundamental and difficult-to-achieve issues [138]. Microfluidic mixing techniques were recently reviewed by Lee et al. [137], Capretto et al. [139], and Suh and Kang [138]. Micromixers that rely on geometrical effects are considered superior for exhibiting chaotic advection over the whole range of the mixing channel.

The special advantage of using IBL in the fabrication of microfluidic mixer devices is to be able to pattern sophisticated three-dimensional channel geometries (see Figure 7) in a single fabrication step [74] (please find the complete mixer device fabrication procedure in the same publication). Moreover, IBL provides unprecedented freedom to produce elaborate, nanoscale designs incorporated in the channel geometry. Full-scale microfluidic devices may be fabricated by conventional methods, and IBL may be employed “mix & match” style, only for creating mixer channels and other applicable parts. Because FIB milling can be done in virtually all solid materials that can serve as molds for replication, and because molding is a widely used technique in microfluidic devices fabrication, IBL enables a potentially low-cost fabrication method that provides complex, custom-designed, nanoscale geometries.

5.15. MEMS Devices. Microelectromechanical systems (MEMS) are microfabricated devices, mostly sensors, such as gyroscopes, accelerometers, or pressure sensors and actuators. FIB techniques such as milling, etching, and deposition are attractive for MEMS processing, because they allow dry and resistless, high resolution patterning that can be applied on already released structures and be placed at various angles, perhaps decorating vertical or curved surfaces. Modifications with the purpose of calibration, specializations, and customizations are frequently done by these methods at R&D laboratories. 3D structures, mostly in the form of deposits, are particularly interesting additions. Apart from modifications, the complete fabrication of small samples of resonant structures such as cantilevers is also often reported by milling in various materials. FIB milling was also proposed as an adoptable last fabrication step for commercial production of electron tunneling based microaccelerometers by Daniel et al. [140], which is also described along with other unique MEMS applications, such

as hermetic encapsulation using FIB deposition, in a review article by Reyntjens and Puers [141].

5.16. Proximal Probes. FIB-based modifications of probes for scanning probe microscopy techniques usually address resolution and sensitivity issues by improving the structure of the very tip. In general, high aspect ratio tips can be fabricated with minimal tip radius of curvature. In the following list we provide some example references:

(i) atomic force microscopy (AFM) [142, 143],

(ii) scanning tunneling microscopy (STM) [143],

(iii) magnetic force microscopy (MFM) [144],

(iv) Kelvin probe force microscopy (KFM) [145],

(v) near-field scanning optical microscopy (NSOM) [146, 147],

(vi) scanning electrochemical microscopy (SECM) [148],

(vii) scanning ion conductance microscopy (SICM) [149].

Scanning probes have also been modified for various lithography procedures such as for nanoindentation lithography [150] and for dip pen lithography [151].

High-aspect ratio probe fabrication by the hard masking technique could enable easier batch fabrication and non-standard probe materials. Silicon [152] and all-diamond [68] probes have been demonstrated by hard masking so far.

5.17. Specimen Preparation for SEM, TEM, APT, or Other Analyses. Specimen preparation for analysis is a widely employed FIB application serving the fields of materials sciences, biosciences, and geosciences, among others. The simplest site-specific FIB procedures for analytical investigations include cross-section milling tasks that are followed by SEM, FIB, or other types of imaging. Repeated milling and imaging is often used as a basis for FIB tomography. A more complicated specimen preparation procedure is needed for transmission electron microscopy and atom probe tomography, for which a region of interest on the sample is identified, removed, and transferred to a suitable support where it is then secured and machined into appropriate shape and size. Surface features as well as buried structures may be prepared. Throughout the procedure the original quality of the sample is maintained by using protective coatings and carefully choosing patterning parameters. These specimen preparation techniques are best done in FIB instruments that feature a 5 or 6 axes eucentric stage and an additional SEM column. Gas injection systems and a micromanipulator (for the sample transfer) are a must. For more about these and sample preparation for other analytical techniques see Langford [153], Mayer et al. [154], and Uchic et al. [155].

5.18. Microtools. Mechanical micromachining is a fabrication method alternative to lithographic approaches, in which miniaturized drilling, grinding, milling, slotting, and other subtractive processes are performed with microtools, especially microcutting tools. The fabrication of microcutting tools by traditional methods is challenging due to the nonplanar microshape of the tool heads (i.e., curved cross-section), whereas FIB manufacturing of microtools (by milling and etching) allows for a large variety of tool shapes and precise, submicron resolution geometries. Cutting tools with dimensions in the 15–100 μm range and cutting edge radii of curvature of 40 nm were demonstrated by Picard et al. [156]. Microsurgical tools and manipulators may also be produced; see Vasile et al. [157] for an example of FIB-fabricated tissue stabilizer used in microsurgical operation.

5.19. Applications in Industry. To mention some of the industry applications we start with the earliest industrial application of FIB technology for photomask repair in the 1980s [19]. While optical mask repair is an off-line operation of the semiconductor industry, it is nevertheless an indispensable service, as making completely defect-free masks is very difficult, especially for the latest lithography needs with ever decreasing line widths [158]. Typical IBL techniques in photomask repair are ion beam assisted deposition and ion beam assisted etching that are used to fill clear defects and etch opaque defects. Nowadays photomask repair is increasingly done by focused electron beams instead of ion beams, with the benefit of less damage in the quartz plate at the site of repair [37].

The characterization and modification of prototype integrated circuit devices, as well as physical failure analysis that serves a production line, are long pursued FIB applications in the industry. Rewiring interconnects for circuit editing or selectively deprocessing a certain chip area for investigating a defective component is a routine procedure today [37, 159]. These techniques employ gas injection systems for selective milling of materials, or for etching at a higher rate and removing larger volumes, or for deposition of conductive and insulating strips as needed. End-point detection techniques are critical. Micromanipulators may be used for *in situ* electrical measurements and for easy failure localization by active voltage contrast imaging. Defect analysis may also require FIB specimen preparation for high resolution electron microscopy.

The hard disk drive manufacturing industry introduced FIB technology in their production line in the late 1990s for the trimming of magnetic write heads. While read-write heads are fabricated mainly by optical lithography, an additional wafer-scale FIB milling step is employed to shape the magnetic strip used for writing. For more, see Athas et al. [160], Koshikawa et al. [161], and Khizroev et al. [162].

6. Conclusion

In summary, we have presented a general overview of techniques for maskless focused ion beam lithography and their applications in micro- and nanofabrication. Our paper suffices as a short but comprehensive tutorial for many interested readers, and it may serve and is mostly arranged as a quick reference guide. It is kindly recommended that readers follow the references for extensive discussions of the various topics at any point. We have introduced the physical nature

of FIB patterning based on ion and matter interactions and have linked these physical phenomena to their application in the fabrication process. This was followed by a review of the main instrumentation components and features and in particular the requirements that a dedicated ion beam lithography instrument has to meet. The introduced specifications of instrument performance such as beam diameter or pattern resolution and other important aspects like system stability and pattern placement accuracy also reflect these requirements. We have finished the instrumentation section with an overview of ion source concepts and ion species in the light of micro- and nanofabrication, as it is a trend to look at alternative ion beams to gallium. Another section was dedicated to the introduction of IBL processing parameters and to the most important IBL patterning concepts such as field stitching and pattern overlay. Given the complexity of the ion-sample interactions and the patterning process, we have listed main fabrication challenges (covering milling in particular) and provided possible causes and solutions for minimizing unintended effects. Select IBL techniques are discussed in the last section and a brief introduction to many applications is provided here, in an attempt to list most types of currently pursued IBL applications for the reader.

Direct-write ion beam lithography titles a rapidly expanding group of IBL techniques that were introduced in this paper. The most distinctive feature of FIB is its capability of machining any material by surface erosion, and FIB has been widely applied to microtechnology and metrology for this reason [1]. Nanofabrication by thin film milling is also very popular in various applications. However, other, less-conventional IBL techniques deserve our attention. In particular, processes with high ion sensitivity carry the possibility of a relatively high processing speed, paving the way to new nanofabrication methods. For example, low ion dose created surface defects may serve as nucleation sites for directed self-assembly processes, low-dose surface amorphization may help produce regions of distinctively different material properties, intermixing type patterning may allow for finely controlled modification of multilayered thin film structures, and ion implantation with FIB for hard masking may mature to be a widely applicable ultrahigh resolution lithography method. There are many more notable examples introduced in Section 5, where IBL techniques emerge as nanofabrication capabilities, and the list is expected to grow as new ion species (Au, Si, Ge, and more) become widely available for lithography (where the ion source properties allow for the required instrument performance, as discussed in Section 3).

Ion beam lithography instruments that are built to serve FIB-based nanofabrication needs are invaluable tools in this exploration. Superior ion probe beam profiles and large sample/wafer capability with superior reproducibility and accuracy are a must, enabling ultra high resolution work as well as the integration of IBL with other micro- and nanofabrication processes. Indeed, IBL techniques can partner well with other lithography techniques, providing complementary processes. Such mix & match fabrication takes advantage of unique IBL techniques while allowing minimal processing for increased throughput. In Section 5 we have listed many examples where mix & match can be applied; 3D milling of templates for microfluidic devices is one of those. In this case, IBL technology could enable a new generation of microfluidic devices featuring finely designed microchannel walls and precisely shaped submicron channels where needed. Some other developing IBL techniques such as templating for directed self-assembly and master fabrication for nanoimprint also benefit immensely from a dedicated lithography instrument setup, as these fabrication methods (DSA and nanoimprint) are currently in the scope for possible use in semiconductor processing (see the 2011 report of the International Technology Roadmap for Semiconductors, under Lithography).

While only a few commercial applications currently exist, many IBL techniques are applied on a daily basis in research laboratories worldwide. We must agree with Dr. Tseng [10] that IBL technologies are likely to play a major role in future nanofabrication because of their combined superiority in flexibility, resolution and precision, and because of their combined ability for material addition, removal and modification. The number of different IBL techniques available for nanofabrication in a single instrument today is truly impressive, and our toolset will further expand as exciting new methods are being developed by the growing community with the help of perfected ion beam instruments featuring focused beams of various ion species.

Conflict of Interests

The authors declare that there is no conflict of interests with any trademark or software mentioned in the paper. Sven Bauerdick declares his affiliation with Raith GmbH, a company that manufactures and markets instruments for direct-write ion beam lithography. He contributed to this review article by providing technical descriptions and instrument component requirements in Section 3. The authors evaluate general instrument performance based on the introduced general performance of components; however, they do not present evaluation of any specific instrument in this review. Dr. Bauerdick also contributed to Section 5 by identifying notable applications of direct-write ion beam lithography and by providing detailed information (and figures) for some applications. His contribution was unbiased in as much as is possible with the extent of his expertise. Alexandra Joshi-Imre declares that she has no conflict of interests regarding the publication of this review.

Acknowledgments

The authors thank Tatyana Orlova at the University of Notre Dame Integrated Imaging Facility for reviewing the paper and for her help with reference materials. Leonidas E. Ocola at the Center for Nanoscale Materials at Argonne National Laboratory and Joseph Klingfus at Raith USA are also thankfully acknowledged for reviewing the paper. Regarding the work presented in Figure 6, use of the Center for Nanoscale Materials and the Electron Microscopy Center at Argonne National Laboratory was supported by the US Department

of Energy, Office of Science, Office of Basic Energy Sciences, under Contract no. DE-AC02-06CH11357.

References

[1] F. Watt, A. A. Bettiol, J. A. Van Kan, E. J. Teo, and M. B. H. Breese, "Ion beam lithography and nanofabrication: a review," *International Journal of Nanoscience*, vol. 4, no. 3, pp. 269–286, 2005.

[2] H. D. Wanzenboeck and S. Waid, "Focused ion beam lithography," in *Recent Advances in Nanofabrication Techniques and Applications*, B. Cui, Ed., InTech, Rijeka, Croatia, 2011.

[3] L. A. Giannuzzi and F. A. Stevie, *Introduction to Focused Ion Beams: Instrumentation, Theory, Techniques and Practice*, Springer, Boston, Mass, USA, 2005.

[4] J. F. Ziegler, M. D. Ziegler, and J. P. Biersack, "SRIM—the stopping and range of ions in matter (2010)," *Nuclear Instruments and Methods in Physics Research B*, vol. 268, no. 11-12, pp. 1818–1823, 2010.

[5] J. F. Ziegler, J. P. Biersack, and M. D. Ziegler, *SRIM: The Stopping and Range of Ions in Matter*, LuLu Press, 2008.

[6] C. A. Volkert and A. M. Minor, "Focused ion beam microscopy and micromachining," *Materials Research Society Bulletin*, vol. 32, no. 5, pp. 389–399, 2007.

[7] J. Orloff, M. Utlaut, and L. Swanson, *High Resolution Focused Ion Beams: FIB and Its Applications*, Kluwer Academic/Plenum Publishers, New York, NY, USA, 2003.

[8] H. H. Andersen and H. L. Bay, "Sputtering yield measurements," in *Sputtering by Particle Bombardment I*, vol. 47 of *Topics in Applied Physics*, pp. 145–218, 1981.

[9] J. Gierak, "Focused ion beam technology and ultimate applications, topical review," *Semiconductor Science and Technology*, vol. 24, no. 4, Article ID 043001, 2009.

[10] A. A. Tseng, "Recent developments in nanofabrication using focused ion beams," *Small*, vol. 1, no. 10, pp. 924–939, 2005.

[11] O. Wilhelmi and J. J. L. Mulders, "Focused ion beam and dualbeam technology applied to nanoprototyping," in *Nanofabrication Using Focused Ion and Electron Beams Principles and Applications*, I. Utke, S. Moshkalev, and P. Russell, Eds., Oxford University Press, New York, NY, USA, 2012.

[12] S. Tan, R. Livengood, Y. Greenzweig, Y. Drezner, and D. Shima, "Probe current distribution characterization technique for focused ion beam," *Journal of Vacuum Science & Technology B*, vol. 30, no. 6, p. 06F606, 2012.

[13] G. B. Assayag, C. Vieu, J. Gierak, P. Sudraud, and A. Corbin, "New characterization method of ion current-density profile based on damage distribution of Ga^+ focused-ion beam implantation in GaAs," *Journal of Vacuum Science & Technology B*, vol. 11, p. 2420, 1993.

[14] J. Orloff, "High-resolution focused ion beams," *Review of Scientific Instruments*, vol. 64, no. 5, pp. 1105–1130, 1993.

[15] J. Orloff, L. W. Swanson, M. Utlaut et al., "Fundamental limits to imaging resolution for focused ion beams," *Journal of Vacuum Science & Technology B*, vol. 14, no. 6, pp. 3759–3763, 1996.

[16] B. Schmidt, L. Bischoff, J. Teichert et al., "Writing FIB implantation and subsequent anisotropic wet chemical etching for fabrication of 3D structures in silicon," *Sensors and Actuators A*, vol. 61, no. 1–3, pp. 369–373, 1997.

[17] J. Gierak, A. Madouri, A. L. Biance et al., "Sub-5 nm FIB direct patterning of nanodevices," *Microelectronic Engineering*, vol. 84, no. 5–8, pp. 779–783, 2007.

[18] R. L. Seliger and W. P. Fleming, "Focused ion beams in microfabrication," *Journal of Applied Physics*, vol. 45, no. 3, pp. 1416–1422, 1974.

[19] J. Melngailis, "Focused ion beam technology and applications," *Journal of Vacuum Science & Technology B*, vol. 5, no. 2, pp. 469–495, 1987.

[20] J. Orloff, *Handbook of Charged Particle Optics*, Taylor & Francis Group, Boca Raton, Fla, USA, 2nd edition, 2009.

[21] J. J. Van Es, J. Gierak, R. G. Forbes et al., "An improved gallium liquid metal ion source geometry for nanotechnology," *Microelectronic Engineering*, vol. 73-74, pp. 132–138, 2004.

[22] L. Bischoff, "Application of mass-separated focused ion beams in nano-technology," *Nuclear Instruments and Methods in Physics Research B*, vol. 266, no. 8, pp. 1846–1851, 2008.

[23] B. R. Appleton, S. Tongay, M. Lemaitre et al., "Materials modifications using a multi-ion beam processing and lithography system," *Nuclear Instruments and Methods in Physics Research B*, vol. 272, pp. 153–157, 2012.

[24] J. Gierak, A. Madouri, E. Bourhis, L. Travers, D. Lucot, and J. C. Harmand, "Focused gold ions beam for localized epitaxy of semiconductor nanowires," *Microelectronic Engineering*, vol. 87, no. 5–8, pp. 1386–1390, 2010.

[25] D. Winston, B. M. Cord, B. Ming et al., "Scanning-helium-ion-beam lithography with hydrogen silsesquioxane resist," *Journal of Vacuum Science & Technology B*, vol. 27, no. 6, pp. 2702–2706, 2009.

[26] V. Sidorkin, E. Van Veldhoven, E. Van Der Drift, P. Alkemade, H. Salemink, and D. Maas, "Sub-10-nm nanolithography with a scanning helium beam," *Journal of Vacuum Science & Technology B*, vol. 27, no. 4, pp. L18–L20, 2009.

[27] W.-D. Li, W. Wu, and R. S. Williams, "Combined helium ion beam and nanoimprint lithography attains 4 nm half-pitch dense patterns," *Journal of Vacuum Science & Technology B*, vol. 30, no. 6, article 06F304, 2012.

[28] D. Winston, V. R. Manfrinato, S. M. Nicaise et al., "Neon ion beam lithography," *Nano Letters*, vol. 11, no. 10, pp. 4343–4347, 2011.

[29] N. S. Smith, W. P. Skoczylas, S. M. Kellogg et al., "High brightness inductively coupled plasma source for high current focused ion beam applications," *Journal of Vacuum Science & Technology B*, vol. 24, no. 6, pp. 2902–2906, 2006.

[30] C. E. Otis, A. Graupera, D. Laur, S. Zhang, S. Kellogg, and G. Schwind, "Mass filtered plasma focused ion beam system," *Journal of Vacuum Science & Technology B*, vol. 30, no. 6, article 06F604, 2012.

[31] J. L. Hanssen, E. A. Dakin, J. J. McClelland, and M. Jacka, "Using laser-cooled atoms as a focused ion beam source," *Journal of Vacuum Science & Technology B*, vol. 24, no. 6, pp. 2907–2910, 2006.

[32] A. V. Steele, B. Knuffman, J. J. McClelland, and J. Orloff, "Focused chromium ion beam," *Journal of Vacuum Science & Technology B*, vol. 28, no. 6, article C6F1, 2010.

[33] F. Ullmann, F. Grossmann, V. P. Ovsyannikov et al., "Production of noble gas ion beams in a focused ion beam machine using an electron beam ion trap," *Journal of Vacuum Science & Technology B*, vol. 25, no. 6, pp. 2162–2167, 2007.

[34] R. Livengood, S. Tan, Y. Greenzweig, J. Notte, and S. McVey, "Subsurface damage from helium ions as a function of dose, beam energy, and dose rate," *Journal of Vacuum Science & Technology B*, vol. 27, no. 6, pp. 3244–3249, 2009.

[35] A. Imre, L. E. Ocola, L. Rich, and J. Klingfus, "Large area direct-write focused ion-beam lithography with a dual-beam microscope," *Journal of Vacuum Science & Technology B*, vol. 28, no. 2, pp. 304–309, 2010.

[36] A. A. Tseng, "Recent developments in micromilling using focused ion beam technology," *Journal of Micromechanics and Microengineering*, vol. 14, no. 4, pp. R15–R34, 2004.

[37] I. Utke, P. Hoffmann, and J. Melngailis, "Gas-assisted focused electron beam and ion beam processing and fabrication," *Journal of Vacuum Science & Technology B*, vol. 26, no. 4, pp. 1197–1276, 2008.

[38] R. M. Langford, "Focused ion beam nanof abri cat ion: a comparison with conventional processing techniques," *Journal of Nanoscience and Nanotechnology*, vol. 6, no. 3, pp. 661–668, 2006.

[39] J. Gierak, E. Bourhis, G. Faini et al., "Exploration of the ultimate patterning potential achievable with focused ion beams," *Ultramicroscopy*, vol. 109, no. 5, pp. 457–462, 2009.

[40] V. Repain, J.-P. Jamet, N. Vernier et al., "Magnetic interactions in dot arrays with perpendicular anisotropy," *Journal of Applied Physics*, vol. 95, no. 5, pp. 2614–2618, 2004.

[41] J. Gierak, D. Mailly, P. Hawkes et al., "Exploration of the ultimate patterning potential achievable with high resolution focused ion beams," *Applied Physics A*, vol. 80, no. 1, pp. 187–194, 2005.

[42] R. Hull, J. A. Floro, M. Gherasimova et al., "Bridging the length scales between lithographic patterning and self assembly mechanisms in fabrication of semiconductor nanostructure arrays," *Journal of Physics*, vol. 209, Article ID 012003, 2010.

[43] F. Ghaleh, R. Köster, H. Hövel et al., "Controlled fabrication of nanopit patterns on a graphite surface using focused ion beams and oxidation," *Journal of Applied Physics*, vol. 101, no. 4, Article ID 044301, 2007.

[44] P. Mélinon, A. Hannour, L. Bardotti et al., "Ion beam nanopatterning in graphite: characterization of single extended defects," *Nanotechnology*, vol. 19, no. 23, Article ID 235305, 2008.

[45] B. Prével, L. Bardotti, S. Fanget et al., "Gold nanoparticle arrays on graphite surfaces," *Applied Surface Science*, vol. 226, no. 1–3, pp. 173–177, 2004.

[46] A. Hannour, L. Bardotti, B. Prével et al., "2D arrays of CoPt nanocluster assemblies," *Surface Science*, vol. 594, no. 1–3, pp. 1–11, 2005.

[47] I. C. Marcus, I. Berbezier, A. Ronda et al., "In-plane epitaxial growth of self-assembled ge nanowires on Si substrates patterned by a focused ion beam," *Crystal Growth & Design*, vol. 11, no. 7, pp. 3190–3197, 2011.

[48] C. Uzan-Saguy, C. Cytermann, R. Brener, V. Richter, M. Shaanan, and R. Kalish, "Damage threshold for ion-beam induced graphitization of diamond," *Applied Physics Letters*, vol. 67, p. 1194, 1995.

[49] N. R. Parikh, J. D. Hunn, E. McGucken et al., "Single-crystal diamond plate liftoff achieved by ion implantation and subsequent annealing," *Applied Physics Letters*, vol. 61, no. 26, pp. 3124–3126, 1992.

[50] P. Olivero, S. Rubanov, P. Reichart et al., "Ion-beam-assisted lift-off technique for three-dimensional micromachining of freestanding single-crystal diamond," *Advanced Materials*, vol. 17, no. 20, pp. 2427–2430, 2005.

[51] T. N. T. Thi, B. Fernandez, D. Eon et al., "Ultra-smooth single crystal diamond surfaces resulting from implantation and lift-off processes," *Physica Status Solidi A*, vol. 208, no. 9, pp. 2057–2061, 2011.

[52] S. Rubanov and A. Suvorova, "Ion implantation in diamond using 30 keV Ga^+ focused ion beam," *Diamond and Related Materials*, vol. 20, no. 8, pp. 1160–1164, 2011.

[53] W. R. McKenzie, M. Z. Quadir, M. H. Gass, and P. R. Munroe, "Focused ion beam implantation of diamond," *Diamond and Related Materials*, vol. 20, no. 8, pp. 1125–1128, 2011.

[54] A. M. Zaitsev, "Carbon nanowires made on diamond surface by focused ion beam," *Physica Status Solidi A*, vol. 202, no. 10, pp. R116–R118, 2005.

[55] M. A. Draganski, E. Finkman, B. C. Gibson, B. A. Fairchild, and K. Ganesan, "Tailoring the optical constants of diamond by ion implantation," *Optical Materials Express*, vol. 2, no. 5, pp. 644–649, 2012.

[56] S. Tongay, M. Lemaitre, J. Fridmann, A. F. Hebard, B. P. Gila, and B. R. Appleton, "Drawing graphene nanoribbons on SiC by ion implantation," *Applied Physics Letters*, vol. 100, no. 7, Article ID 073501, 2012.

[57] M. G. Lemaitre, "Low-temperature, site selective graphitization of SiC via ion implantation and pulsed laser annealing," *Applied Physics Letters*, vol. 100, Article ID 193105, 2012.

[58] R. L. Kubena, J. W. Ward, F. P. Stratton, R. J. Joyce, and G. M. Atkinson, "A low magnification focused ion beam system with 8 nm spot size," *Journal of Vacuum Science & Technology B*, vol. 9, no. 6, pp. 3079–3083, 1991.

[59] L. Bruchhaus, S. Bauerdick, L. Peto, U. Barth, A. Rudzinski, and J. Mussmann, "High resolution and high density ion beam lithography employing HSQ resist," *Microelectronic Engineering*, vol. 97, pp. 48–50, 2012.

[60] S. Matsui, Y. Kojima, Y. Ochiai, and T. Honda, "High-resolution focused ion beam lithography," *Journal of Vacuum Science & Technology B*, vol. 9, no. 5, p. 2622, 1991.

[61] K. Arshak, M. Mihov, A. Arshak, D. McDonagh, and D. Sutton, "Focused ion beam lithography-overview and new approaches," in *Proceedings of the 24th International Conference on Microelectronics (MIEL '04)*, vol. 2, pp. 459–462, Niš, Serbia, May 2004.

[62] K. Arshak, M. Mihov, S. Nakahara, A. Arshak, and D. McDonagh, "A novel focused-ion-beam lithography process for sub-100 nanometer technology nodes," *Superlattices and Microstructures*, vol. 36, no. 1–3, pp. 335–343, 2004.

[63] K. Arshak, S. F. Gilmartin, D. Collins, O. Korostynska, A. Arshak, and M. Mihov, "Ion beam lithography and resist processing for nanofabrication," in *Proceedings of the Materials Research Society Symposium*, vol. 983, pp. 0983-LL01–0983-LL02, Boston, Mass, USA, December 2006.

[64] J. Xu and A. J. Steckl, "Fabrication of visibly photoluminescent Si microstructures by focused ion beam implantation and wet etching," *Applied Physics Letters*, vol. 65, no. 16, pp. 2081–2083, 1994.

[65] N. Chekurov, K. Grigoras, A. Peltonen, S. Franssila, and I. Tittonen, "The fabrication of silicon nanostructures by local gallium implantation and cryogenic deep reactive ion etching," *Nanotechnology*, vol. 20, no. 6, Article ID 065307, 2009.

[66] M. D. Henry, M. J. Shearn, B. Chhim, and A. Scherer, "Ga^+ beam lithography for nanoscale silicon reactive ion etching," *Nanotechnology*, vol. 21, no. 24, Article ID 245303, 2010.

[67] W. McKenzie, J. Pethica, and G. Cross, "A direct-write, resistless hard mask for rapid nanoscale patterning of diamond," *Diamond and Related Materials*, vol. 20, no. 5-6, pp. 707–710, 2011.

[68] S. K. Tripathi, D. Scanlan, N. O'Hara et al., "Resolution, masking capability and throughput for direct-write, ion implant mask

patterning of diamond surfaces using ion beam lithography," *Journal of Micromechanics and Microengineering*, vol. 22, no. 5, Article ID 055005, 2012.

[69] H.-Y. Lee and H.-B. Chung, "Ga^+ focused-ion-beam exposure and CF_4 reactive-ion-etching development of Si_3N_4 resist optimized by Monte Carlo simulation," *Journal of Vacuum Science & Technology B*, vol. 16, pp. 1161–1166, 1998.

[70] H.-Y. Lee and H.-B. Chung, "Dry-etching development characteristics of $Se_{75}Ge_{25}$ resist for focused-ion-beam lithography," *Journal of Vacuum Science & Technology B*, vol. 16, no. 4, pp. 1987–1991, 1998.

[71] A. Plech, P. Leiderer, and J. Boneberg, "Femtosecond laser near field ablation," *Laser & Photonics Reviews*, vol. 3, no. 5, pp. 435–451, 2009.

[72] M. Deubel, G. von Freymann, M. Wegener, S. Pereira, K. Busch, and C. M. Soukoulis, "Direct laser writing of three-dimensional photonic-crystal templates for telecommunications," *Nature Materials*, vol. 3, pp. 444–447, 2004.

[73] J. Fischer and M. Wegener, "Three-dimensional direct laser writing inspired by stimulated-emission-depletion microscopy," *Optical Materials Express*, vol. 1, no. 4, pp. 614–624, 2011.

[74] E. Palacios, L. E. Ocola, A. Joshi-Imre, S. Bauerdick, M. Berse, and L. Peto, "Three-dimensional microfluidic mixers using ion beam lithography and micromachining," *Journal of Vacuum Science & Technology B*, vol. 28, no. 6, p. C611, 2010.

[75] G. Lalev, P. Petkov, N. Sykes et al., "Fabrication and validation of fused silica NIL templates incorporating different length scale features," *Microelectronic Engineering*, vol. 86, no. 4–6, pp. 705–708, 2009.

[76] J. Kettle, R. T. Hoyle, R. M. Perks, and S. Dimov, "Overcoming material challenges for replication of "motheye lenses" using step and flash imprint lithography for optoelectronic applications," *Journal of Vacuum Science & Technology B*, vol. 26, no. 5, pp. 1794–1799, 2008.

[77] J. Taniguchi, K. Koga, Y. Kogo, and I. Miyamoto, "Rapid and three-dimensional nanoimprint template fabrication technology using focused ion beam lithography," *Microelectronic Engineering*, vol. 83, no. 4–9, pp. 940–943, 2006.

[78] J. Edel and T. Albrecht, *Nanopores for Bioanalytical Applications: Proceedings of the International Conference*, The Royal Society of Chemistry Publishing, London, UK, 2012.

[79] C. Dekker, "Solid-state nanopores," *Nature Nanotechnology*, vol. 2, no. 4, pp. 209–215, 2007.

[80] K. Healy, B. Schiedt, and I. P. Morrison, "Solid-state nanopore technologies for nanopore-based DNA analysis," *Nanomedicine*, vol. 2, no. 6, pp. 875–897, 2007.

[81] R. Mulero, A. S. Prabhu, K. J. Freedman, and M. J. Kim, "Nanopore-based devices for bioanalytical applications," *Journal of Laboratory Automation*, vol. 15, no. 3, pp. 243–252, 2010.

[82] D. Japrung, J. Dogan, K. J. Freedman, A. Nadzeyka, and S. Bauerdick, "Single-molecule studies of intrinsic disordered proteins using solid-state nanopores," *Analytical Chemistry*, vol. 85, no. 4, pp. 2449–2456, 2013.

[83] A. L. Lattes, S. C. Munroe, M. M. Seaver, J. E. Murguia, and J. Melngailis, "Improved drift in two-phase, long-channel, shallow buried-channel CCDs with longitudinally nonuniform storage-gate implants," *IEEE Transactions on Electron Devices*, vol. 39, no. 7, pp. 1772–1774, 1992.

[84] C.-C. Shen, J. Murguia, N. Goldsman, M. Peckerar, J. Melngailis, and D. A. Antoniadis, "Use of focused-ion-beam and modeling to optimize submicron MOSFET characteristics," *IEEE Transactions on Electron Devices*, vol. 45, no. 2, pp. 453–459, 1998.

[85] R. M. Langford, P. M. Nellen, J. Gierak, and Y. Fu, "Focused ion beam micro- and nanoengineering," *Materials Research Society Bulletin*, vol. 32, no. 5, pp. 417–423, 2007.

[86] A. J. De Marco and J. Melngailis, "Maskless fabrication of JFETs via focused ion beams," *Solid-State Electronics*, vol. 48, no. 10-11, pp. 1833–1836, 2004.

[87] T. Shinada, S. Okamoto, T. Kobayashi, and I. Ohdomari, "Enhancing semiconductor device performance using ordered dopant arrays," *Nature*, vol. 437, no. 7062, pp. 1128–1131, 2005.

[88] M. Hori, T. Shinada, K. Taira et al., "Performance enhancement of semiconductor devices by control of discrete dopant distribution," *Nanotechnology*, vol. 20, no. 36, Article ID 365205, 2009.

[89] P. M. Koenraad and M. E. Flatté, "Single dopants in semiconductors," *Nature Materials*, vol. 10, no. 2, pp. 91–100, 2011.

[90] J. C. McCallum, D. N. Jamieson, C. Yang et al., "Single-ion implantation for the development of Si-based MOSFET devices with quantum functionalities," *Advances in Materials Science and Engineering*, vol. 2012, Article ID 272694, 10 pages, 2012.

[91] C. Meier, D. Reuter, C. Riedesel, and A. D. Wieck, "Fabrication of two-dimensional electron systems by focused ion beam doping of III/V semiconductor heterostructures," *Journal of Applied Physics*, vol. 93, no. 10, pp. 6100–6106, 2003.

[92] D. G. Deppe and N. Holonyak Jr., "Atom diffusion and impurity-induced layer disordering in quantum well III-V semiconductor heterostructures," *Journal of Applied Physics*, vol. 64, no. 12, pp. R93–R113, 1988.

[93] A. J. Steckl, P. Chen, H. E. Jackson et al., "Review of focused ion beam implantation mixing for the fabrication of GaAs-based optoelectronic devices," *Journal of Vacuum Science & Technology B*, vol. 13, no. 6, pp. 2570–2575, 1995.

[94] H. König, N. Mais, E. Höfling et al., "Focused ion beam implantation for opto- and microelectronic devices," *Journal of Vacuum Science & Technology B*, vol. 16, no. 4, pp. 2562–2566, 1998.

[95] J. P. Reithmaier and A. Forchel, "Focused ion-beam implantation induced thermal quantum-well intermixing for monolithic optoelectronic device integration," *IEEE Journal on Selected Topics in Quantum Electronics*, vol. 4, no. 4, pp. 595–605, 1998.

[96] V. Aimez, J. Beauvais, J. Beerens, D. Morris, H. S. Lim, and B.-S. Ooi, "Low-energy ion-implantation-induced quantum-well intermixing," *IEEE Journal on Selected Topics in Quantum Electronics*, vol. 8, no. 4, pp. 870–879, 2002.

[97] G. H. Waller, A. Stein, and J. T. Abiade, "Nanofabrication of doped, complex oxides," *Journal of Vacuum Science & Technology B*, vol. 30, no. 1, Article ID 011804, 2012.

[98] I. Vrejoiu, M. Alexe, D. Hesse, and U. Gösele, "Functional perovskites—from epitaxial films to nanostructured arrays," *Advanced Functional Materials*, vol. 18, no. 24, pp. 3892–3906, 2008.

[99] J. A. Klug, M. V. Holt, R. N. Premnath et al., "Elastic relaxation and correlation of local strain gradients with ferroelectric domains in (001) $BiFeO_3$ nanostructures," *Applied Physics Letters*, vol. 99, no. 5, Article ID 052902, 2011.

[100] S. Avci, Z. L. Xiao, J. Hua et al., "Matching effect and dynamic phases of vortex matter in $Bi_2Sr_2CaCu_2O_8$ nanoribbon with a periodic array of holes," *Applied Physics Letters*, vol. 97, no. 4, Article ID 042511, 2010.

[101] M. L. Latimer, Z. L. Xiao, J. Hua, A. Joshi-Imre, and Y. L. Wang, "Anisotropy of the critical temperature of a superconducting

niobium thin film with an array of nanoscale holes in an external magnetic field," *Physical Review B*, vol. 87, no. 2, Article ID 020507, 2013.

[102] E. S. Sadki, S. Ooi, and K. Hirata, "Focused-ion-beam-induced deposition of superconducting nanowires," *Applied Physics Letters*, vol. 85, no. 25, pp. 6206–6208, 2004.

[103] J. C. Lodder, "Patterned Nanomagnetic Films," in *Advanced Magnetic Nanostructures*, pp. 261–288, Springer, New York, NY, USA, 2006, ISBN 9780387233093.

[104] S. Khizroev and D. Litvinov, "Focused-ion-beam-based rapid prototyping of nanoscale magnetic devices," *Nanotechnology*, vol. 15, no. 3, pp. R7–R15, 2004.

[105] A. Lapicki, K. Kang, and T. Suzuki, "Fabrication of magnetic dot arrays by ion beam induced chemical vapor deposition (IBICVD)," *IEEE Transactions on Magnetics*, vol. 38, no. 5, part 1, pp. 2589–2591, 2002.

[106] A. Lapicki, E. Ahmad, and T. Suzuki, "Ion beam induced chemical vapor deposition (IBICVD) of cobalt particles," *Journal of Magnetism and Magnetic Materials*, vol. 240, no. 1–3, pp. 47–49, 2002.

[107] Q. Y. Xu, Y. Kageyama, and T. Suzuki, "Ion-beam-induced chemical-vapor deposition of FePt and CoPt particles," *Journal of Applied Physics*, vol. 97, no. 10, Article ID 10K308, 2005.

[108] J. Fassbender and J. McCord, "Magnetic patterning by means of ion irradiation and implantation," *Journal of Magnetism and Magnetic Materials*, vol. 320, no. 3-4, pp. 579–596, 2008.

[109] M. G. Blaber, M. D. Arnold, and M. J. Ford, "A review of the optical properties of alloys and intermetallics for plasmonics," *Journal of Physics*, vol. 22, no. 14, p. 143201, 2010.

[110] W. L. Barnes, A. Dereux, and T. W. Ebbesen, "Surface plasmon subwavelength optics," *Nature*, vol. 424, no. 6950, pp. 824–830, 2003.

[111] W. A. Murray and W. L. Barnes, "Plasmonic materials," *Advanced Materials*, vol. 19, no. 22, pp. 3771–3782, 2007.

[112] Y. Fu, F. Fang, and Z. Xu, "Nanofabrication and characterization of plasmonic structures," in *Nanofabrication*, Y. Masuda, Ed., chapter 9, InTech, Rijeka, Croatia, 2011.

[113] J. T. Bahns, A. Imre, V. K. Vlasko-Vlasov et al., "Enhanced Raman scattering from focused surface plasmons," *Applied Physics Letters*, vol. 91, no. 8, Article ID 081104, 2007.

[114] L. Rosa, K. Sun, V. Mizeikis, S. Bauerdick, L. Peto, and S. Juodkazis, "3D-tailored gold nanoparticles for light field enhancement and harvesting over visible-IR spectral range," *Journal of Physical Chemistry C*, vol. 115, no. 13, pp. 5251–5256, 2011.

[115] I. Chyr and A. J. Steckl, "Focused ion beam micromachining of GaN photonic devices," *Materials Research Society Proceedings*, vol. 537, article G10.7, 1999.

[116] N. A. Paraire, P. G. Filloux, and K. Wang, "Patterning and characterization of 2D photonic crystals fabricated by focused ion beam etching of multilayer membranes," *Nanotechnology*, vol. 15, no. 3, pp. 341–346, 2004.

[117] D. Freeman, S. Madden, and B. Luther-Davies, "Fabrication of planar photonic crystals in a chalcogenide glass using a focused ion beam," *Optics Express*, vol. 13, no. 8, pp. 3079–3086, 2005.

[118] Y. K. Kim, A. J. Danner, J. J. Raftery, and K. D. Choquette, "Focused ion beam nanopatterning for optoelectronic device fabrication," *IEEE Journal on Selected Topics in Quantum Electronics*, vol. 11, no. 6, pp. 1292–1297, 2005.

[119] M. J. Cryan, M. Hill, D. C. Sanz et al., "Focused ion beam-based fabrication of nanostructured photonic devices," *IEEE Journal on Selected Topics in Quantum Electronics*, vol. 11, no. 6, pp. 1266–1276, 2005.

[120] S. Cabrini, L. Businaro, M. Prasciolu et al., "Focused ion beam fabrication of one-dimensional photonic crystals on Si_3N_4/SiO_2 channel waveguides," *Journal of Optics A*, vol. 8, no. 7, pp. S550–S553, 2006.

[121] W. C. L. Hopman, F. Ay, W. Hu et al., "Focused ion beam scan routine, dwell time and dose optimizations for submicrometre period planar photonic crystal components and stamps in silicon," *Nanotechnology*, vol. 18, no. 19, Article ID 195305, 2007.

[122] F. Ay, I. Iñurrategui, D. Geskus, S. Aravazhi, and M. Pollnau, "Integrated lasers in crystalline double tungstates with focused-ion-beam nanostructured photonic cavities," *Laser Physics Letters*, vol. 8, no. 6, pp. 423–430, 2011.

[123] F. Ay, K. Wörhoff, and R. M. de Ridder, "Focused-ion-beam nanostructuring of AI_2O_3 dielectric layers for photonic applications," *Journal of Micromechanics and Microengineering*, vol. 22, no. 10, Article ID 105008, 2012.

[124] S. Juodkazis, L. Rosa, S. Bauerdick, L. Peto, R. El-Ganainy, and S. John, "Sculpturing of photonic crystals by ion beam lithography: towards complete photonic bandgap at visible wavelengths," *Optics Express*, vol. 19, no. 7, pp. 5802–5810, 2011.

[125] Y.-Q. Fu, N. Kok, and A. Bryan, "Microfabrication of microlens array by focused ion beam technology," *Microelectronic Engineering*, vol. 54, no. 3-4, pp. 211–221, 2000.

[126] T. M. Babinec, J. T. Choy, K. J. M. Smith, M. Khan, and M. Lončar, "Design and focused ion beam fabrication of single crystal diamond nanobeam cavities," *Journal of Vacuum Science & Technology B*, vol. 29, no. 1, Article ID 010601, 2011.

[127] I. Bayn, B. Meyler, A. Lahav et al., "Processing of photonic crystal nanocavity for quantum information in diamond," *Diamond and Related Materials*, vol. 20, no. 7, pp. 937–943, 2011.

[128] A. D. Greentree, B. A. Fairchild, F. M. Hossain, and S. Prawer, "Diamond integrated quantum photonics," *Materials Today*, vol. 11, no. 9, pp. 22–31, 2008.

[129] H.-H. Tao, R. Cheng, F. Shuai, and Z.-Y. Li, "Optical improvement of photonic devices fabricated by Ga^+ focused ion beam micromachining," *Journal of Vacuum Science & Technology B*, vol. 25, no. 5, pp. 1609–1614, 2007.

[130] J. Schrauwen, F. Van Laere, D. Van Thourhout, and R. Baets, "Focused-ion-beam fabrication of slanted grating couplers in silicon-on-insulator waveguides," *IEEE Photonics Technology Letters*, vol. 19, no. 11, pp. 816–818, 2007.

[131] F. Schiappelli, R. Kumar, M. Prasciolu et al., "Efficient fiber-to-waveguide coupling by a lens on the end of the optical fiber fabricated by focused ion beam milling," *Microelectronic Engineering*, vol. 73-74, pp. 397–404, 2004.

[132] W. Yuan, F. Wang, and O. Bang, "Optical fiber sensors fabricated by the focused ion beam technique," in *22nd International Conference on Optical Fiber Sensors*, vol. 8421 of *Proceedings of SPIE*, Beijing, China, October 2012.

[133] J. Huang, A. Alqahtani, J. Viegas, and M. S. Dahlem, "Fabrication of optical fiber gratings through focused ion beam techniques for sensing applications," in *Proceedings of the Photonics Global Conference (PGC '12)*, pp. 1–4, Singapore, December 2012.

[134] K. Keskinbora, C. Grévent, M. Bechtel, M. Weigand, and E. Goering, "Ion beam lithography for Fresnel zone plates in X-ray microscopy," *Optics Express*, vol. 21, no. 10, pp. 11747–11756, 2013.

[135] A. Nadzeyka, L. Petoa, S. Bauerdick et al., “Ion beam lithography for direct patterning of high accuracy large area X-ray elements in gold on membranes,” *Microelectronic Engineering*, vol. 98, pp. 198–201, 2012.

[136] P. P. Ilinski, B. P. Lai, N. J. Bassom, J. Donald, and G. J. Athas, “X-ray zone plate fabrication using a focused ion beam,” in *Advances in X-Ray Optics*, vol. 4145 of *Proceedings of SPIE*, pp. 311–316, The International Society for Optical Engineering, San Diego, Calif, USA, July 2000.

[137] C.-Y. Lee, C.-L. Chang, Y.-N. Wang, and L.-M. Fu, “Microfluidic mixing: a review,” *International Journal of Molecular Sciences*, vol. 12, no. 5, pp. 3263–3287, 2011.

[138] Y. K. Suh and S. Kang, “A review on Mixing in Microfluidics,” *Micromachines*, vol. 1, no. 3, pp. 82–111, 2010.

[139] L. Capretto, W. Cheng, M. Hill, and X. Zhang, “Micromixing within microfluidic devices,” *Topics in Current Chemistry*, vol. 304, pp. 27–68, 2011.

[140] J. H. Daniel, D. F. Moore, and J. F. Walker, “Focused ion beams for microfabrication,” *Engineering Science and Education Journal*, vol. 7, no. 2, pp. 53–56, 1998.

[141] S. Reyntjens and R. Puers, “A review of focused ion beam applications in microsystem technology,” *Journal of Micromechanics and Microengineering*, vol. 11, no. 4, pp. 287–300, 2001.

[142] M. J. Vasile, D. Grigg, J. E. Griffith, E. Fitzgerald, and P. E. Russell, “Scanning probe tip geometry optimized for metrology by focused ion beam ion milling,” *Journal of Vacuum Science & Technology B*, vol. 9, no. 6, p. 3569, 1991.

[143] B. G. Konoplev, O. A. Ageev, V. A. Smirnov, A. S. Kolomiitsev, and N. I. Serbu, “Probe modification for scanning probe microscopy by the focused ion beam method,” *Russian Microelectronics*, vol. 41, no. 1, pp. 41–50, 2012.

[144] L. Gao, L. P. Yue, T. Yokota et al., “Focused ion beam milled CoPt magnetic force microscopy tips for high resolution domain images,” *IEEE Transactions on Magnetics*, vol. 40, no. 4, pp. 2194–2196, 2004.

[145] K. Akiyama, T. Eguchi, T. An, Y. Fujikawa, T. Sakurai, and Y. Hasegawa, “Functional probes for scanning probe microscopy,” *Journal of Physics*, vol. 61, no. 1, article 5, pp. 22–25, 2007.

[146] S. Pilevar, K. Edinger, W. Atia, I. Smolyaninov, and C. Davis, “Focused ion-beam fabrication of fiber probes with well-defined apertures for use in near-field scanning optical microscopy,” *Applied Physics Letters*, vol. 72, no. 24, pp. 3133–3135, 1998.

[147] E. X. Jin and X. Xu, “Focussed ion beam machined cantilever aperture probes for near-field optical imaging,” *Journal of Microscopy*, vol. 229, no. 3, pp. 503–511, 2008.

[148] A. Avdic, A. Lugstein, M. Wu et al., “Fabrication of cone-shaped boron doped diamond and gold nanoelectrodes for AFM-SECM,” *Nanotechnology*, vol. 22, no. 14, Article ID 145306, 2011.

[149] D. J. Comstock, J. W. Elam, M. J. Pellin, and M. C. Hersam, “Integrated ultramicroelectrode-nanopipet probe for concurrent scanning electrochemical microscopy and scanning Ion conductance microscopy,” *Analytical Chemistry*, vol. 82, no. 4, pp. 1270–1276, 2010.

[150] C. Menozzi, L. Calabri, P. Facci, P. Pingue, F. Dinelli, and P. Baschieri, “Focused ion beam as tool for atomic force microscope (AFM) probes sculpturing,” *Journal of Physics*, vol. 126, Article ID 012070, 2008.

[151] X. Wang, L. Vincent, D. Bullen, J. Zou, and C. Liu, “Scanning probe lithography tips with spring-on-tip designs: analysis, fabrication, and testing,” *Applied Physics Letters*, vol. 87, no. 5, Article ID 054102, 2005.

[152] G. Villanueva, J. A. Plaza, A. Sánchez-Amores et al., “Deep reactive ion etching and focused ion beam combination for nanotip fabrication,” *Materials Science and Engineering C*, vol. 26, no. 2-3, pp. 164–168, 2006.

[153] R. M. Langford, “Focused ion beams techniques for nanomaterials characterization,” *Microscopy Research and Technique*, vol. 69, no. 7, pp. 538–549, 2006.

[154] J. Mayer, L. A. Giannuzzi, T. Kamino, and J. Michael, “TEM sample preparation and FIB-induced damage,” *Materials Research Society Bulletin*, vol. 32, no. 5, pp. 400–407, 2007.

[155] M. D. Uchic, L. Holzer, B. J. Inkson, E. L. Principe, and P. Munroe, “Three-dimensional microstructural characterization using focused ion beam tomography,” *Materials Research Society Bulletin*, vol. 32, no. 5, pp. 408–416, 2007.

[156] Y. N. Picard, D. P. Adams, M. J. Vasile, and M. B. Ritchey, “Focused ion beam-shaped microtools for ultra-precision machining of cylindrical components,” *Precision Engineering*, vol. 27, no. 1, pp. 59–69, 2003.

[157] M. J. Vasile, R. Nassar, J. Xie, and H. Guo, “Microfabrication techniques using focused ion beams and emergent applications,” *Micron*, vol. 30, no. 3, pp. 235–244, 1999.

[158] A. Yasaka, F. Aramaki, M. Muramatsu et al., “Application of vector scanning in focused ion beam photomask repair system,” *Journal of Vacuum Science & Technology B*, vol. 26, no. 6, pp. 2127–2130, 2008.

[159] C. Boit, R. Schlangen, U. Kerst, and T. Lundquist, “Physical techniques for chip-backside IC debug in nanotechnologies,” *IEEE Design & Test of Computers*, vol. 25, no. 3, pp. 250–257, 2008.

[160] G. J. Athas, K. E. Noll, R. Mello et al., “Focused ion beam system for automated MEMS prototyping and processing,” in *Micromachining and Microfabrication Process Technology III*, vol. 3223 of *Proceedings of SPIE*, pp. 198–207, Austin, Tex, USA, September 1997.

[161] T. Koshikawa, A. Nagai, Y. Yokoyama, and T. Hoshino, “A new write head trimmed at wafer level by focused ion beam,” *IEEE Transactions on Magnetics*, vol. 34, no. 4, pp. 1471–1473, 1998.

[162] S. Khizroev, Y. Liu, K. Mountfield, M. H. Kryder, and D. Litvinov, “Physics of perpendicular magnetic recording: writing process,” *Journal of Magnetism and Magnetic Materials*, vol. 246, no. 1-2, pp. 335–344, 2002.

[163] P. Mazarov, A. D. Wieck, L. Bischoff, and W. Pilz, “Alloy liquid metal ion source for carbon focused ion beams,” *Journal of Vacuum Science & Technology B*, vol. 27, no. 6, pp. L47–L49, 2009.

[164] O. Wilhelmi, S. Reyntjens, C. Mitterbauer, L. Roussel, D. J. Stokes, and D. H. W. Hubert, “Rapid prototyping of nanostructured materials with a focused ion beam,” *Japanese Journal of Applied Physics*, vol. 47, no. 6, pp. 5010–5014, 2008.

[165] D. J. Stokes, T. Vystavel, and F. Morrissey, “Focused ion beam (FIB) milling of electrically insulating specimens using simultaneous primary electron and ion beam irradiation,” *Journal of Physics D*, vol. 40, no. 3, article 028, pp. 874–877, 2007.

Journal of
Nanotechnology

International Journal of
Corrosion

International Journal of
Polymer Science
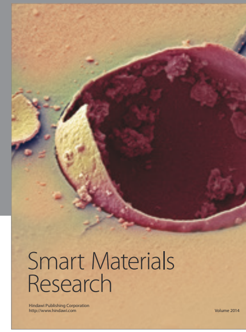
Smart Materials
Research

Journal of
Composites

BioMed
Research International

Hindawi
Submit your manuscripts at
http://www.hindawi.com
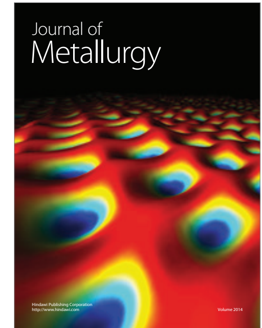
Journal of
Metallurgy

Journal of
Materials
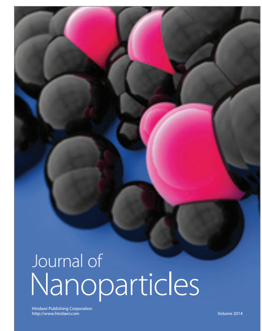
Journal of
Nanoparticles
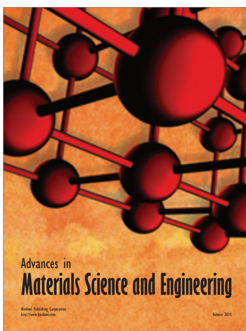
Advances in
Materials Science and Engineering
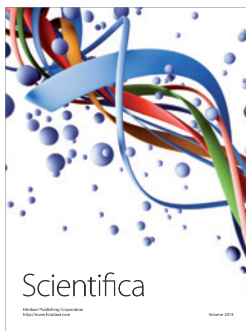
Scientifica
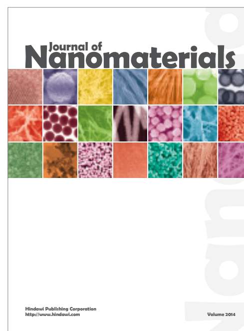
Journal of
Nanomaterials
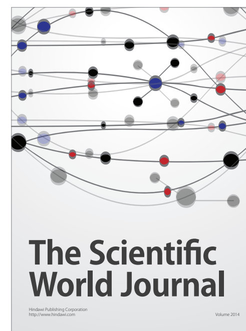
The Scientific
World Journal

International Journal of
Biomaterials

Journal of
Nanoscience

Journal of
Coatings

Journal of
Crystallography

Journal of
Ceramics

Journal of
Textiles